Cosmic Evolution Survey
COSMOS

What can we learn on obscured AGN from the COSMOS Survey

Vincenzo Mainieri
ESO

G. Hasinger, M. Brusa, N. Cappelluti, F. Civano, A. Comastri, F. Fiore, R. Gilli, K. Iwasawa, M. Salvato, J. Silverman, C. Vignali, G. Zamorani

OUTLINE:

- background
- introduction to the COSMOS Survey
    - Counterpart identification
    - Spectroscopic follow-up
- searching for obscured AGN
    - X-ray
    - X-ray + mid-IR
- conclusion and future

What do we know?

- ✦ Unobscured AGN → picture quite clear from optical and soft X-ray surveys (SDSS/ROSAT etc.)
  → Luminosity-Dependent Density Evolution (LDDE)
  see Hasinger, Miyaji, Schmidt 2005

- ✦ Obscured AGN → still large debate on:
  - number density (especially at z~2 – quasar activity peak)
  - ratio obs/unobs
    * well-established only locally (Risaliti et al. 1999)
    * predicted to be 1:1 from unified schemes
    * "needed" 3-4:1 to 10:1 in XRB models (e.g. Gilli et al. 2001/2007)
  - dependence of the ratio obs/unobs on luminosity and/or redshift (see e.g. La Franca et al. 2005/Treister & Urry 2006)

- ✦ Role of the envinronment in triggering nuclear activity --> interplay between galaxy, clusters and dark matter

Still lot of "observational work" to do…

Selection of (compton thin) obscured AGN

Most efficient way: Hard X-ray surveys

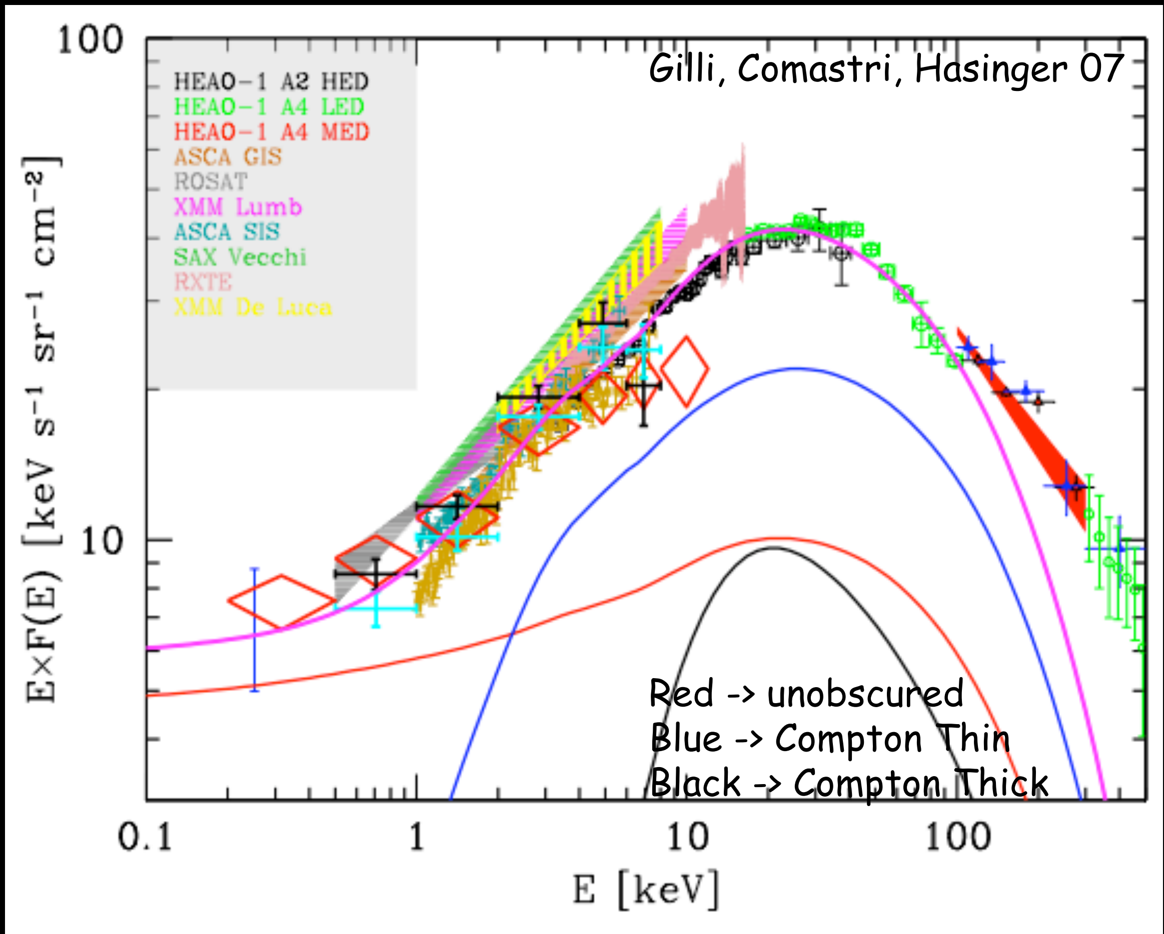

Examples:

high X/O sources and EXOs (moderate obscured AGN at z~1-2 hosted in massive ellipticals, and very high-z)

- Fiore et al. 2003, A&A
- Mignoli et al. 2004, A&A
- Mainieri et al. 2005, A&A
- Maiolino et al. 2006, A&A
- Koekemoer et al. 2004 ApJL
- etc…

CAVEAT:

hard X-ray surveys still miss the highest obscured sources (don't sample the XRB peak) - see Worsley et al. 2005,2006, Comastri 2004 + IR-related works http://cosmos.astro.caltech.edu/

PI N. Scoville

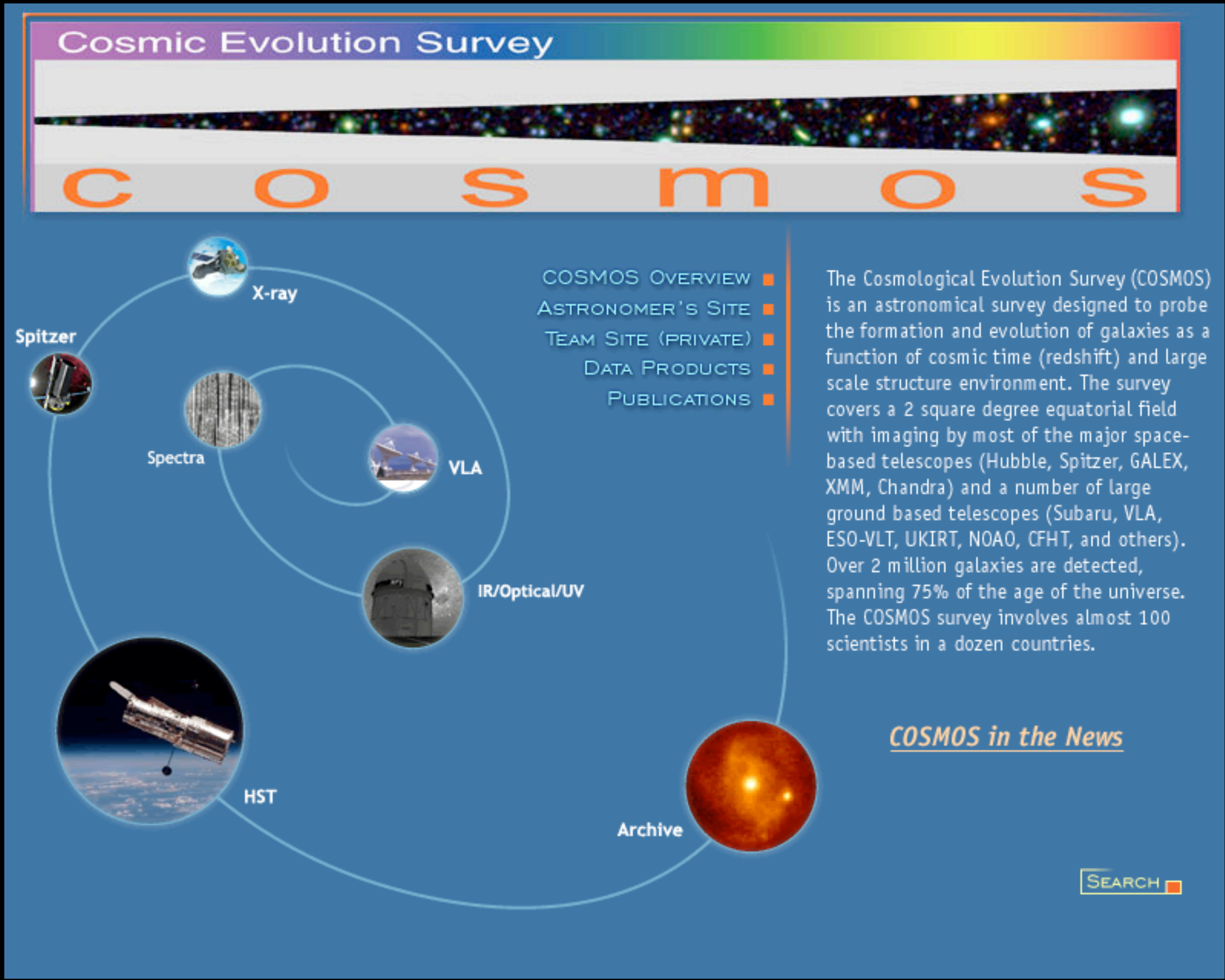

Members of the COSMOS collaboration

PI: Nicholas Scoville (California Institute of Technology, USA/CA)
PM: Bill Green (Pasadena, USA/CA)

Roberto G. Abraham (University of Toronto, Canada)
James Aguirre (University of Colorado at Boulder, USA/CO)
Mr. Masaru Ajiki (Tohuku University, Japan)
Hervé Aussel (AIM, CNRS, France)
Josh E. Barnes (University of Hawaii, USA/HI)
Andrew Benson (California Institute of Technology, USA/CA)
Frank Bertoldi (Radioastronomisches Institut der Universitaet Bonn, Germany)
Andrew Blain (California Institute of Technology, USA/CA)
Marcella Brusa (Max-Planck-Institut fur Extraterrestrische Physik, Germany)
Daniela Calzetti (Space Telescope Science Institute, USA/MD)
Peter Capak (California Institute of Technology, USA/CA)
Chris Carilli (National Radio Astronomy Observatory, USA/NM)
John E. Carlstrom (University of Chicago, USA/IL)
C. Marcella Carollo (Eidgenossiche Technische Hochschule (ETH), Switzerland)
Andrea Cimatti (INAF - Osservatorio Astrofisico di Arcetri, Italy)
Andrea Comastri (INAF - Osservatorio Astronomico di Bologna, Italy)
Thierry Contini (Laboratoire d'Astrophysique de Toulouse et de Tarbes, France)
Emanuele Daddi (European Southern Observatory, Germany)
Richard S. Ellis (California Institute of Technology, USA/CA)
Martin Elvis (Harvard-Smithsonian Center for Astrophysics, USA/MA)
Amr El-Zant (University of Toronto, Canada)
Shawn Ewald (California Institute of Technology, USA/CA)
Michael Fall (Space Telescope Science Institute, USA/MD)
Alexis Finoguenov (Max-Planck-Institut fur Extraterrestrische Physik, Germany)
Alberto Franceschini (University of Padova, Italy)
Mauro Giavalisco (Space Telescope Science Institute, USA/MD)
Richard E. Griffiths (Carnegie Mellon University, USA/PA)
Luigi (Gigi) Guzzo (INAF - Osservatorio di Brera, Milano)
Günther Hasinger (Max-Planck-Institut fur Extraterrestrische Physik, Germany)
Olivier Ilbert (University of Hawaii, USA/HI)
Chris Impey (University of Arizona, USA/AZ)
Knud Jahnke (Max Planck Institut fur Astronomie, Germany)
Ms. Jeyhan Kartaltepe (University of Hawaii, USA/HI)
Ms. Lisa Kewley (University of Hawaii, USA/HI)
Manfred Kitbichler (Max-Planck-Institut fur Astrophysik, Germany)
Jean-Paul Kneib (California Institute of Technology, USA/CA)
Anton Koekemoer (Space Telescope Science Institute, USA/MD)
Oliver Lefevre (Laboratoire d'Astrophysique de Marseille, France)
Simon J. Lilly (Eidgenossiche Technische Hochschule(ETH), Switzerland)
Charles Liu (American Museum of Natural History, USA/NY)
Christian Maier (Eidgenossiche Technische Hochschule (ETH), Switzerland)
Vincenzo Mainieri (European Southern Observatory, Germany)
Eduardo Martin (University of Hawaii, USA/HI)
Richard Massey (California Institute of Technology, USA/CA)
Henry Joy McCracken (CNRS, Institute d'Astrophysique de Paris, France)
Yannick Mellier (CNRS, Institute d'Astrophysique de Paris, France)
Takamitsu Miyaji (Carnegie Mellon University, USA/PA)
Satoshi Miyazaki (Subaru Telescope, NAO, Japan)
Bahram Mobasher (Space Telescope Science Institute, USA/MD)
Jeremy Mould (National Optical Astronomy Observatory, USA/AZ)
Takashi Murayama (Tohoku University, Japan)
Karel Nel (University of Witswatersrand, South Africa)
Colin Norman (Space Telescope Science Institute, USA/MD)
John Peacock (Royal Observatory, Edinburgh, UK)
Cristiano Porciani (Eidgenossiche Technische Hochschule (ETH), Switzerland)
Alexandre Refregier (Commissariat a l'Energie Atomique (CEA), France)
Alvio Renzini (Osservatorio Astronomico di Padova, Italy)
Jason Rhodes (California Institute of Technology, USA/CA)
Michael Rich (University of California at Los Angeles, USA/CA)
Dimitra Rigopoulou (Oxford University, UK)
Mara Salvato (California Institute of Technology, USA/CA)
David B. Sanders (University of Hawaii, USA/HI)
Mr. Shunji Sasaki (Tohoku University, Japan)
Claudia Scarlata (Eidgenossiche Technische Hochschule (ETH), Switzerland)
David Schiminovich (California Institute of Technology, USA/CA)
Eva Schinnerer (Max Planck Institut fur Astronomie, Germany)
Marco Scodeggio (Instituto di Astrofisica Spaziale e Fisica Cosmica, Italy)
Kartik Sheth (California Institute of Technology, USA/CA)
Yasuhiro Shioya (Tohoku University, Japan)
Patrick Shopbell (California Institute of Technology, USA/CA)
John Silverman (Max-Planck-Institut fur Extraterrestrische Physik, Germany)
Mari Takahashi (Tohoku University, Japan)
Yoshi Taniguchi (University of Tokyo, Japan)
Lidia Tasca (Laboratoire d'Astrophysique de Marseille, France)
James Taylor (California Institute of Technology, USA/CA)
Dave Thompson (California Institute of Technology, USA/CA)
Shana Tribiano (CUNY Borough of Manhattan Community College, USA/NY)
Jon Trump (University of Arizona, USA/AZ)
Neil deGrasse Tyson (American Museum of Natural History, USA/NY)
Claudia Megan Urry (Yale University, USA/CT)
Ludovic Van Waerbeke (University of British Columbia, Canada)
Paolo Vettolani (L'Istituto Nazionale di Astrofisica, Italy)
Simon D. M. White (Max-Planck-Institut fur Astrophysik, Germany)
Lin Yan (California Institute of Technology, USA/CA)
Gianni Zamorani (L'Istituto Nazionale di Astrofisica, Bologna, Italy)

Cosmos Survey

2 deg^2 (PI: N. Scoville)

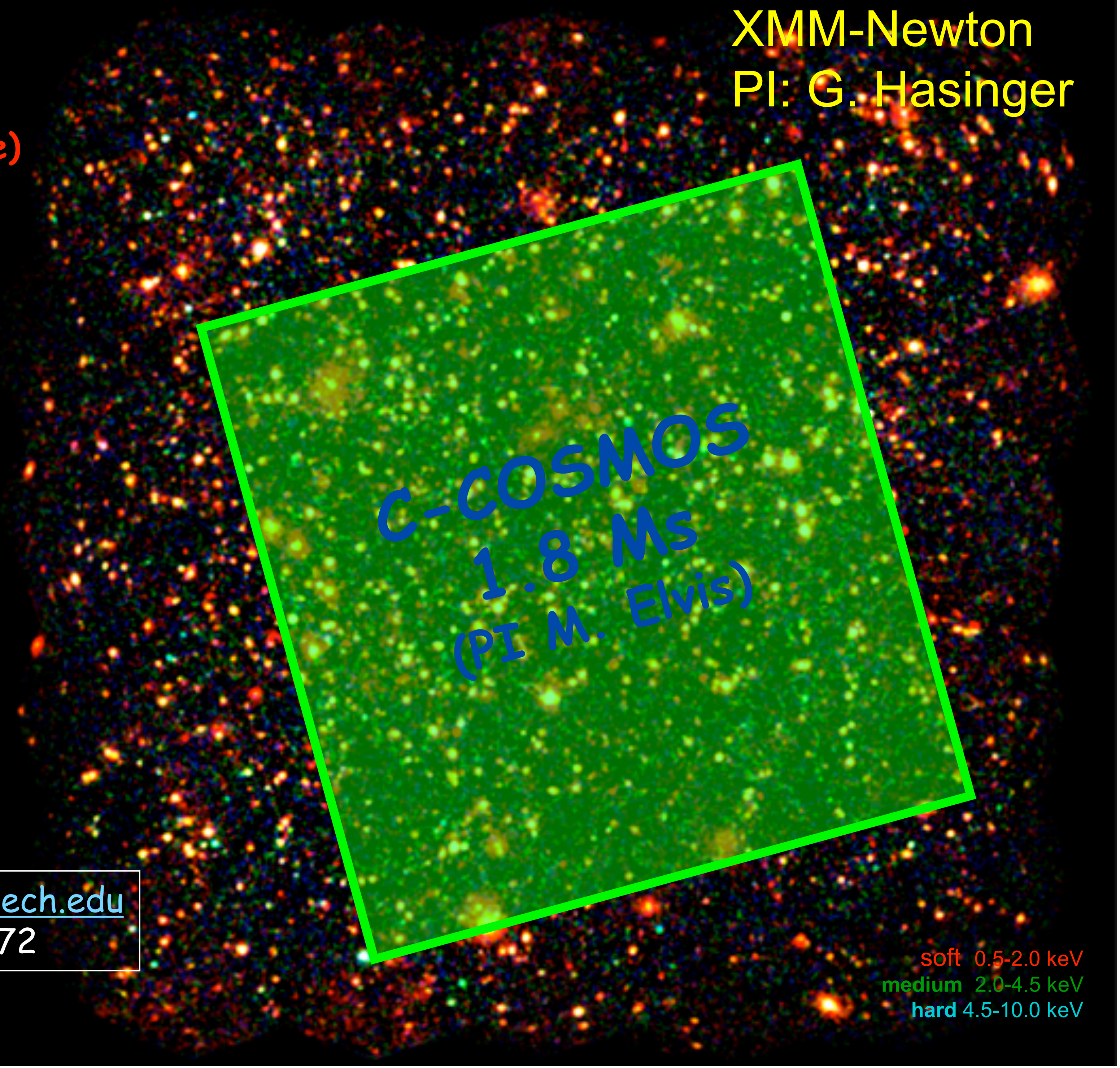

http://cosmos.astro.caltech.edu

ApJS special issue vol. 172

Trieste, Oct 3rd, 200

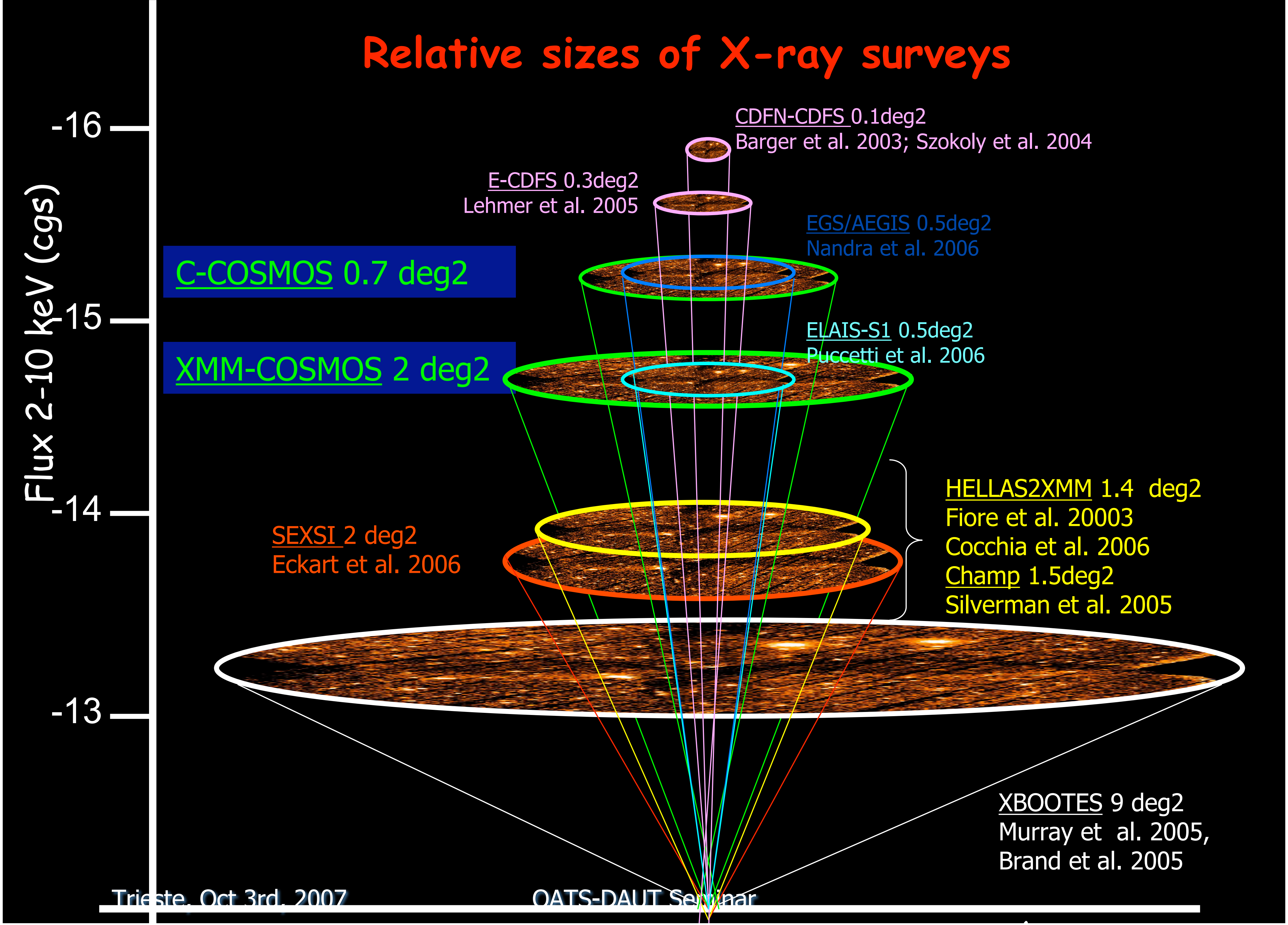
Relative sizes of X-ray surveys
Flux 2-10 keV (cgs)
-16
-15
-14
-13
CDFN-CDFS 0.1deg2
Barger et al. 2003; Szokoly et al. 2004
E-CDFS 0.3deg2
Lehmer et al. 2005
EGS/AEGIS 0.5deg2
Nandra et al. 2006
C-COSMOS 0.7 deg2
XMM-COSMOS 2 deg2
ELAIS-S1 0.5deg2
Puccetti et al. 2006
HELLAS2XMM 1.4 deg2
Fiore et al. 20003
Cocchia et al. 2006
Champ 1.5deg2
Silverman et al. 2005
SEXSI 2 deg2
Eckart et al. 2006
XBOOTES 9 deg2
Murray et al. 2005,
Brand et al. 2005
Trieste, Oct 3rd, 2007
OATS-DAUT Seminar

XMM observations: tiling strategy

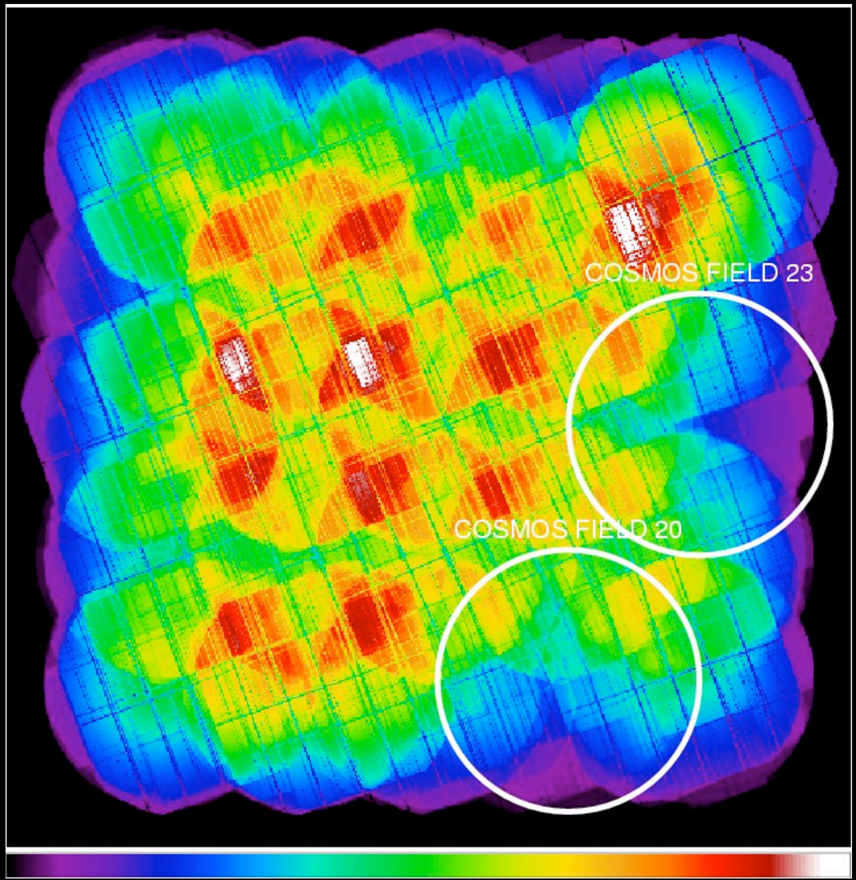

Why 1.4 Ms?

Average 50 ks exposure →
transition between source
and background limited detection
+ not confusion limited

Homogeneous exposure map →
homogeneous limiting flux

→Mosaic of 25 pointings, closely spaced, repeated twice

1) logN-logS and cosmic variance studies
0.5-2 keV logN-logS

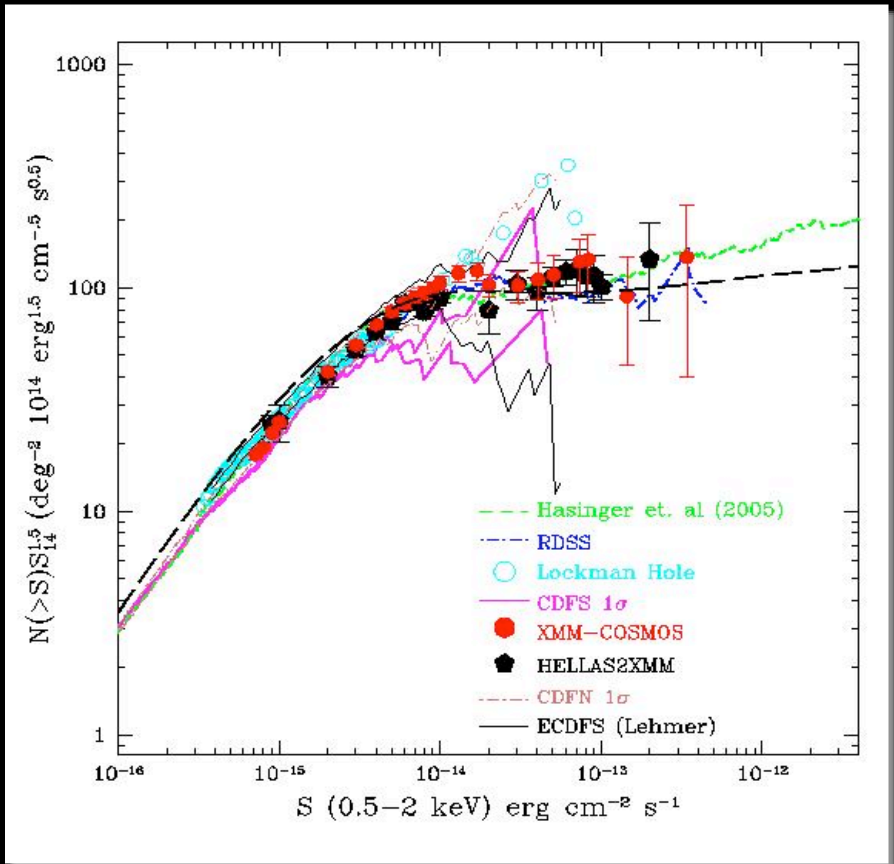

Cappelluti et al. 2007

logN-logS (normalized to Euclidean slope)

→0.5-2 keV
Confirm previous results with unprecedent accuracy in the flux range 8×10^{-16}-5×10^{-12} cgs:

logN-logS and cosmic variance studies
5-10 keV logN-logS

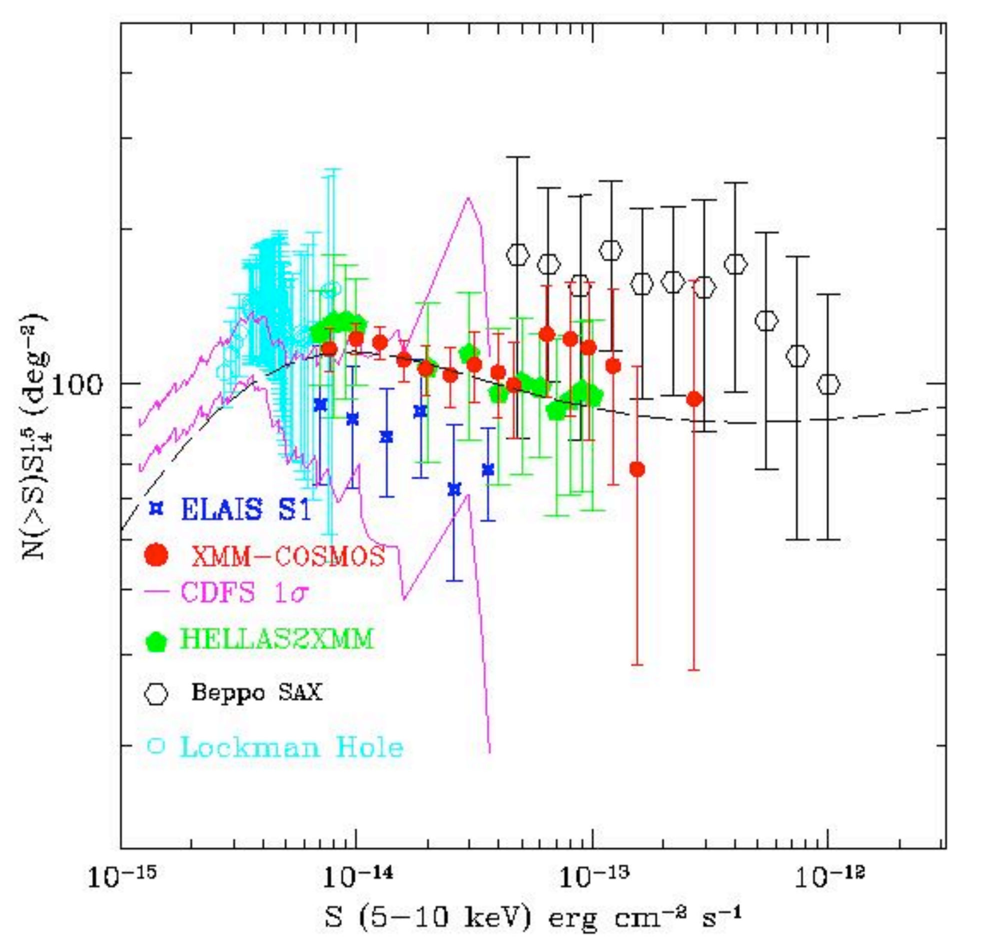

→5-10 keV
[250 sources!]

In between previous determinations in the flux range 8×10^{-15}- 5×10^{-12} cgs and in excellent agreement with models predictions

Cappelluti et al., 2007 (Models by Gilli, Comastri, Hasinger 2007)

X-ray to optical diagram

1865 independent
X-ray sources (5 sigma)

1608 soft (0.5-2 keV)
1103 hard (2-10 keV)
250 very hard (5-10 keV)

Identification status

(based on likelihood ratio technique, K-band/IRAC catalogs, Chandra validation & visual inspection)

-"secure" counterparts
1441 sources (82.4%)

- "ambiguous" counterparts:
298 sources (16.4%)

-"unidentified" sample
21 sources (1.2%)

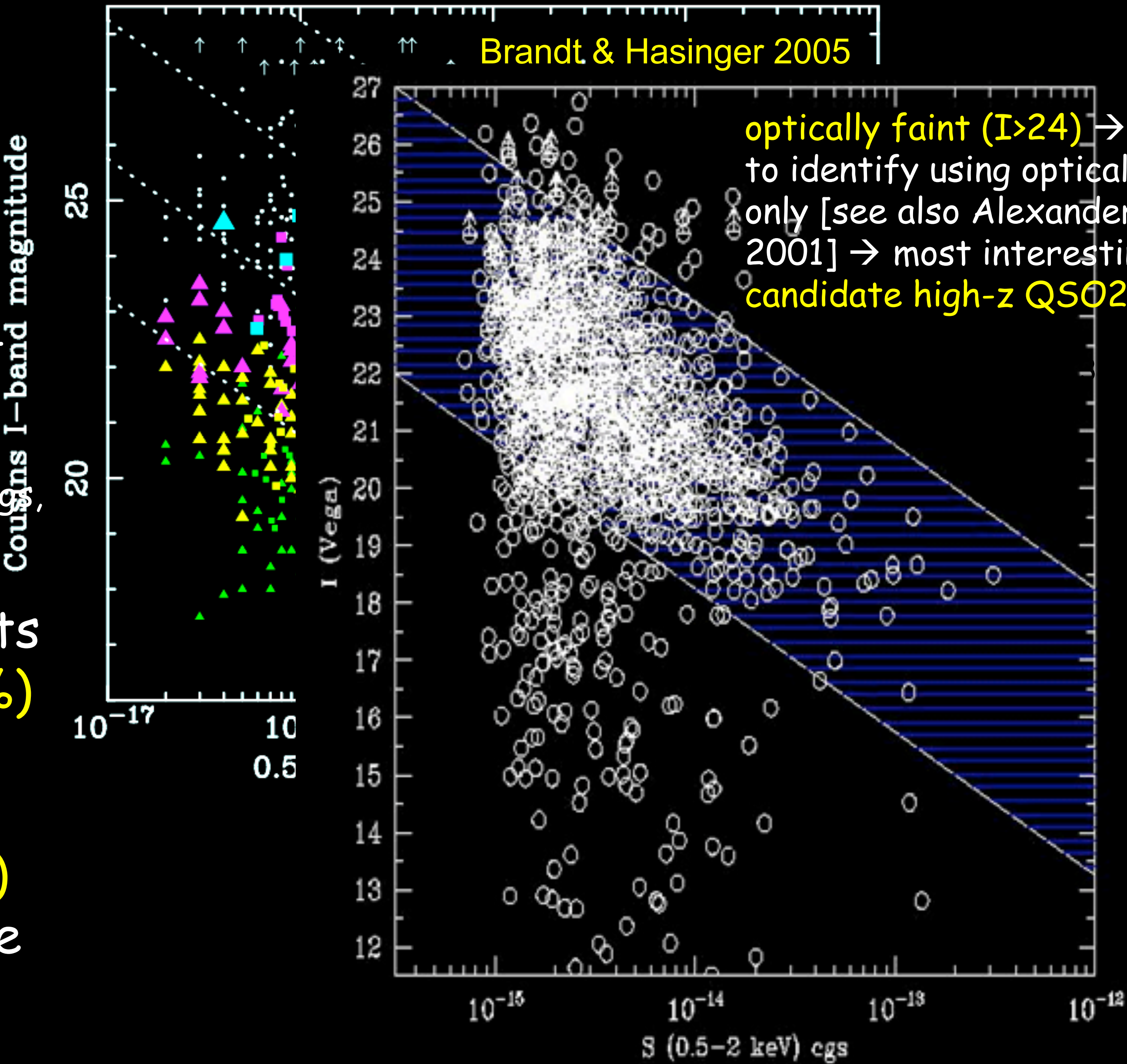

optically faint (I>24) → difficult to identify using optical bands only [see also Alexander et al. 2001] → most interesting sources
candidate high-z QSO2

Examples of XMM/IRAC coincidences
IRAC identified sources

Courtesy: Salvato, Ilbert + S-COSMOS

- ~150 objects in XMM-COSMOS identified through K/IRAC (most of them EROs/red objects/optically faint)
- Very hard to get redshift from optical → alternative approaches: ISAAC/MOIRCS/IRS spectroscopy and/or SED fitting

  [Koekemoer et al. 2004, Mainieri et al. 2005, Maiolino et al. 2006]

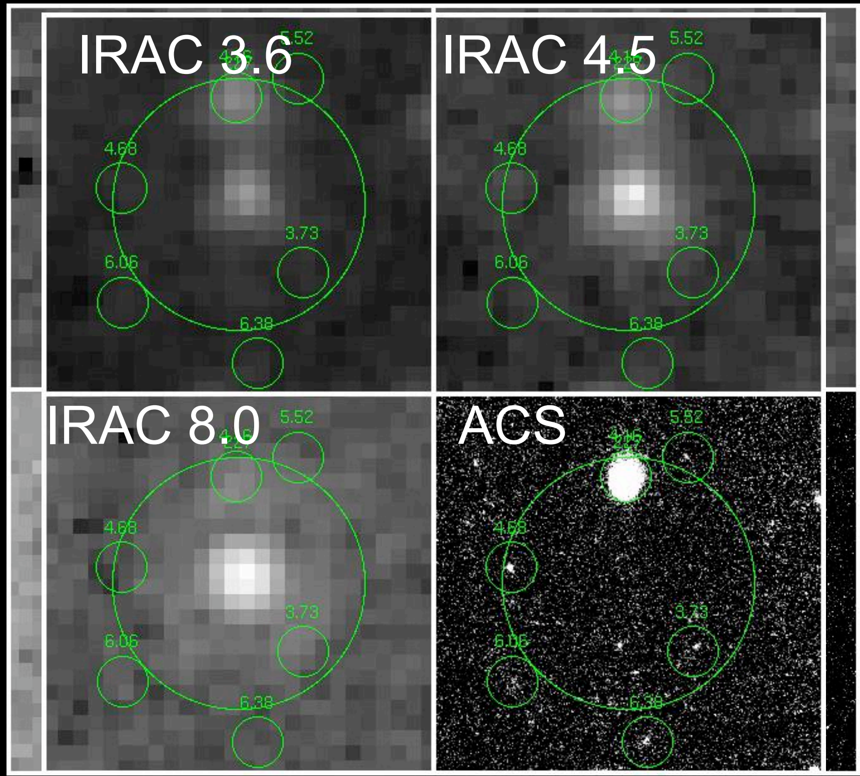

Brusa et al. 2007

Anton's program on SUBARU/MOIRCS!

Examples of XMM/IRAC coincidences on bright/ambiguous sources

- ~300 objects in XMM-COSMOS with multiple/none IRAC cps
  → more accurate X-ray positions needed to pick up the right cp
  → **C-COSMOS → reduced them to ~150 (half area)**

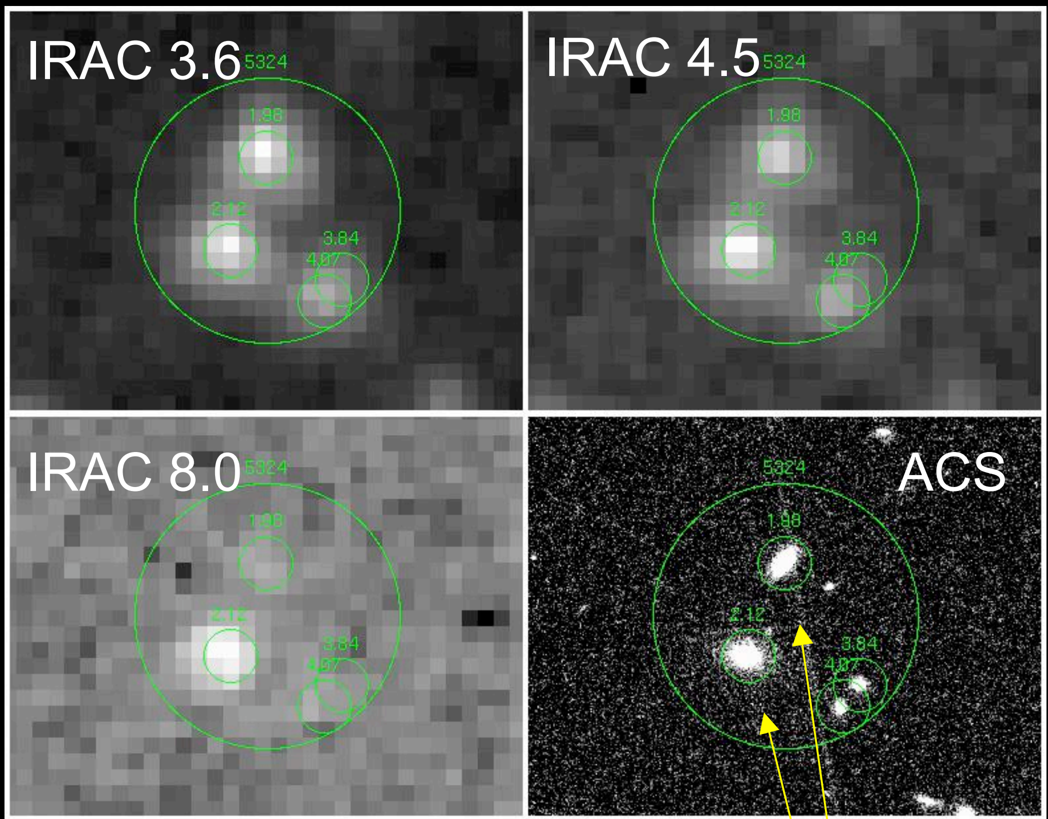

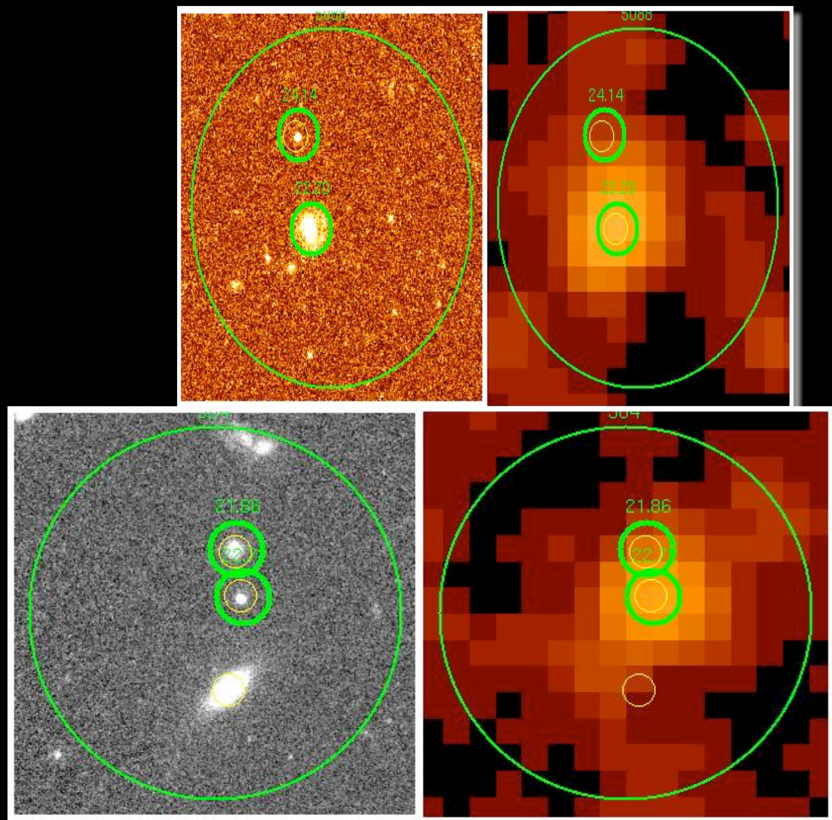

Both can be counterparts
→Try to put BOTH in slits

3) From optical cp to rest-frame properties → Redshifts distributions

compilation from ongoing spectroscopic projects [IMACS/zCOSMOS + SDSS + literature data]

- ~650 "secure" spectroscopic identifications
  [35% of the full sample, almost 50% completeness in the I<22 sample]

- BL AGNs dominate at z>1
  → High redshift type 2 objects missing (partly selection effect)

  [see also results from HELLAS2XMM, Cocchia et al. 2007 and from the SEXSI survey, Eckart et al. 2006]

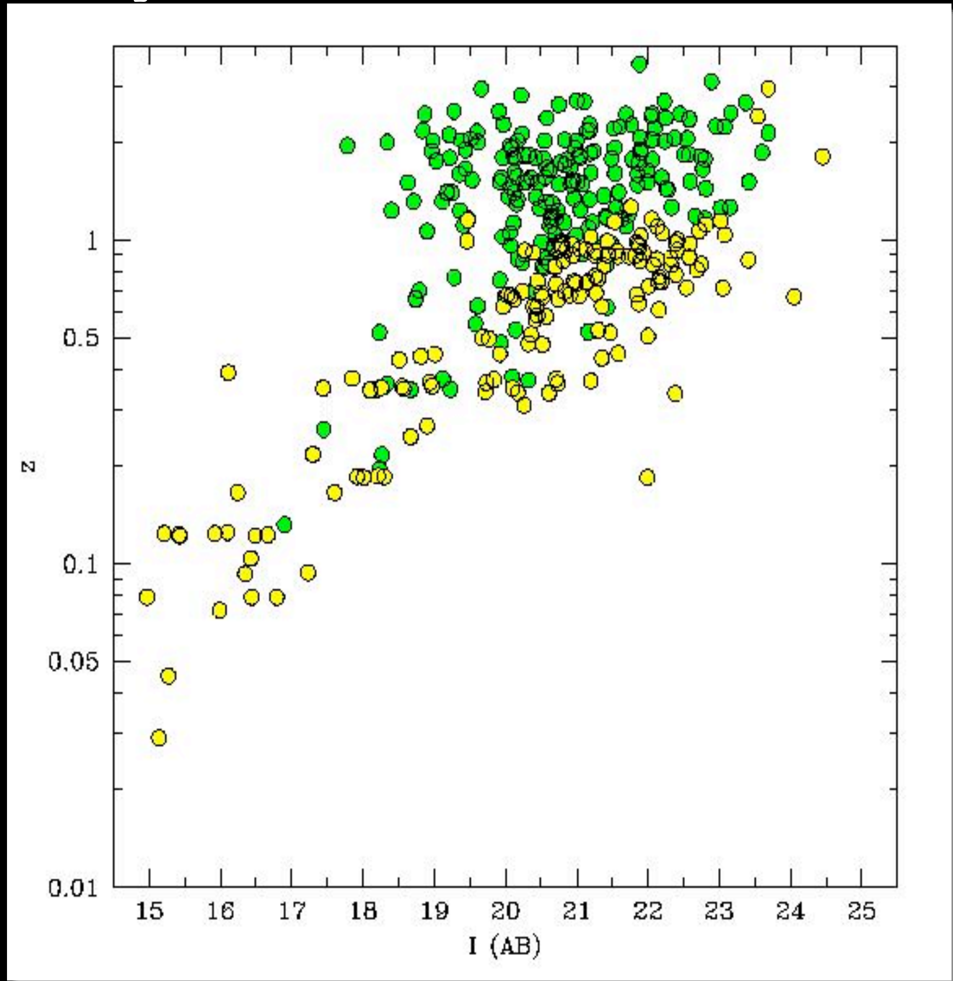

Photometric redshifts for AGN

σ = 0.017

Less than 10% of catastrophic errors

- improved templates, including hybrids of galaxy+AGN
- Photometry from >30 bands (SDSS, Subaru including IB, CFHT, J, K, IRAC)

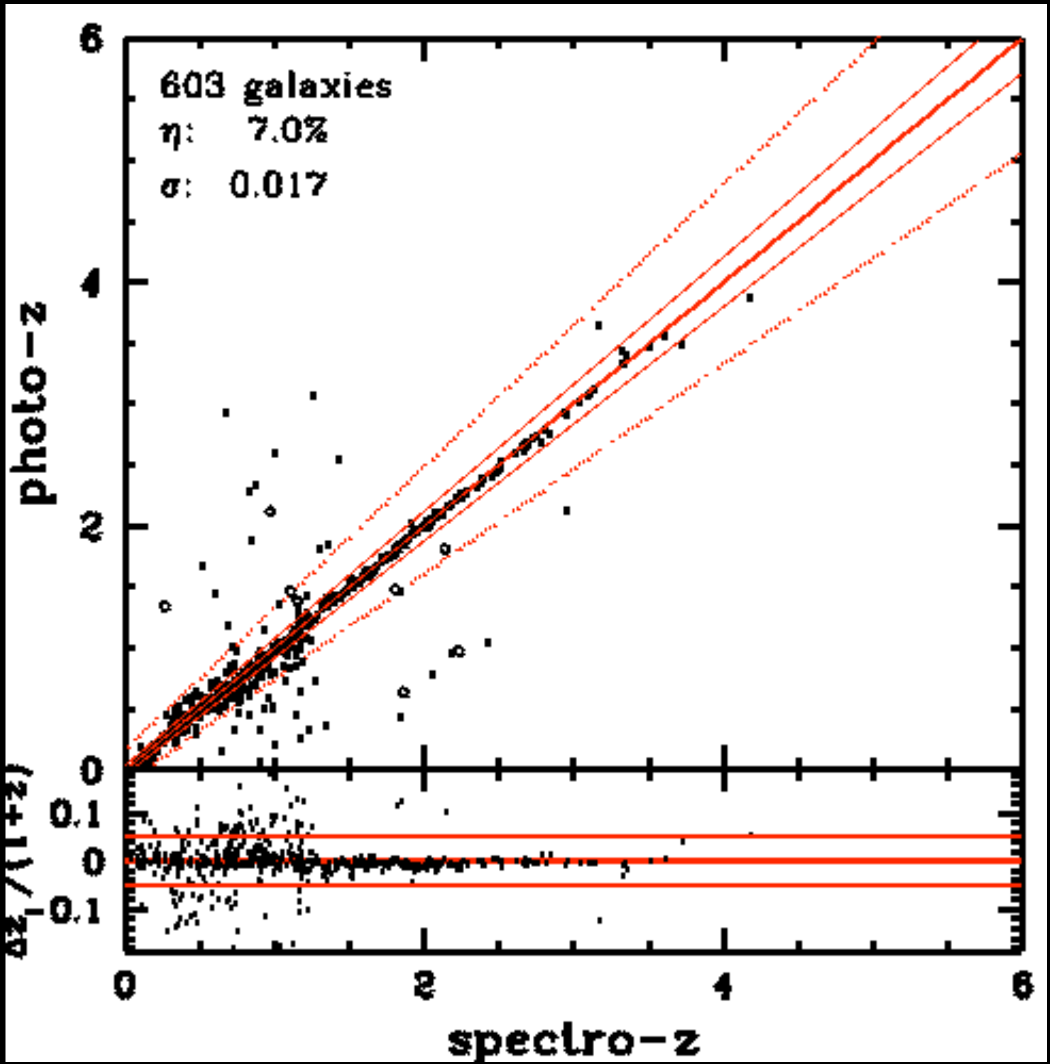

Salvato et al., in prep
using LePhare

The XMM-COSMOS survey (PI G. Hasinger)

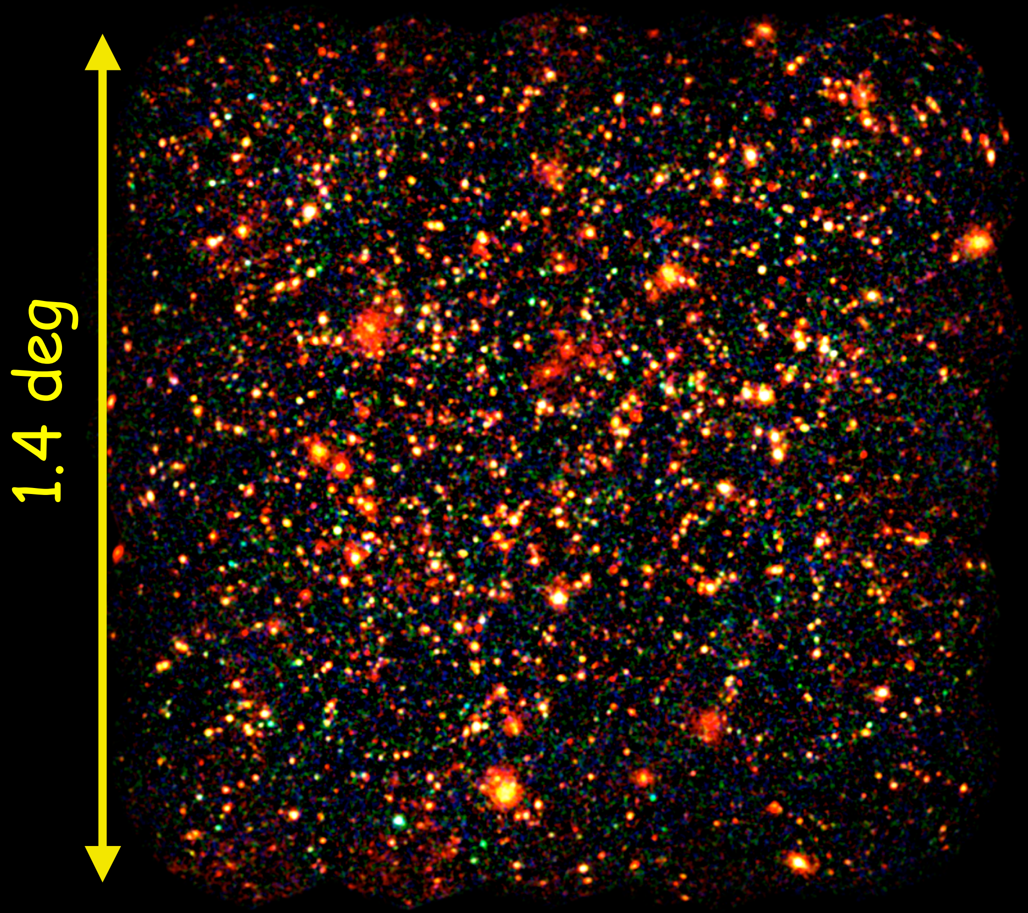

Area = 2 deg^2

Flux limits:

[0.5-2] keV -> 7.0×10^{-16} cgs

[2-10] keV -> 3.3×10^{-15} cgs

[5-10] keV -> 1.0×10^{-14} cgs

~1800 point-like X-ray sources

X-ray spectral analysis:

483 with zspec

900 with zspec or zphot

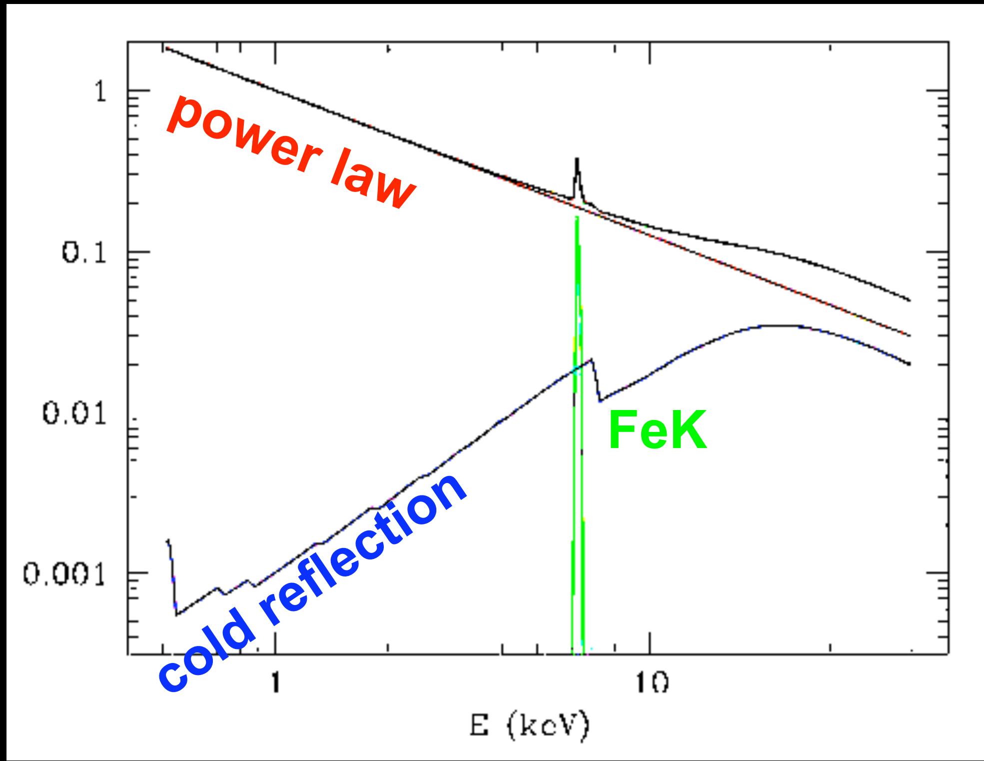

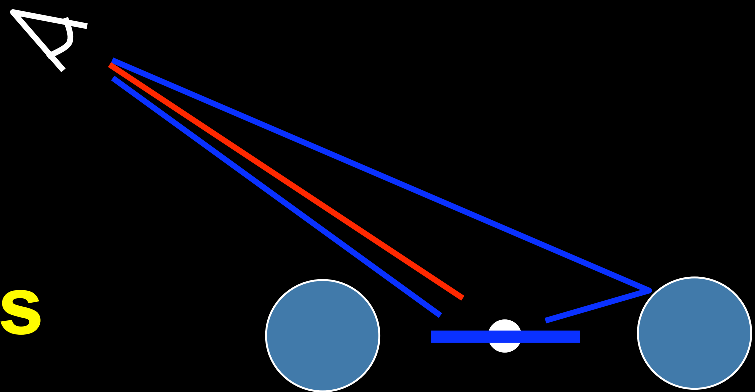

Emission components

by R. Maiolino

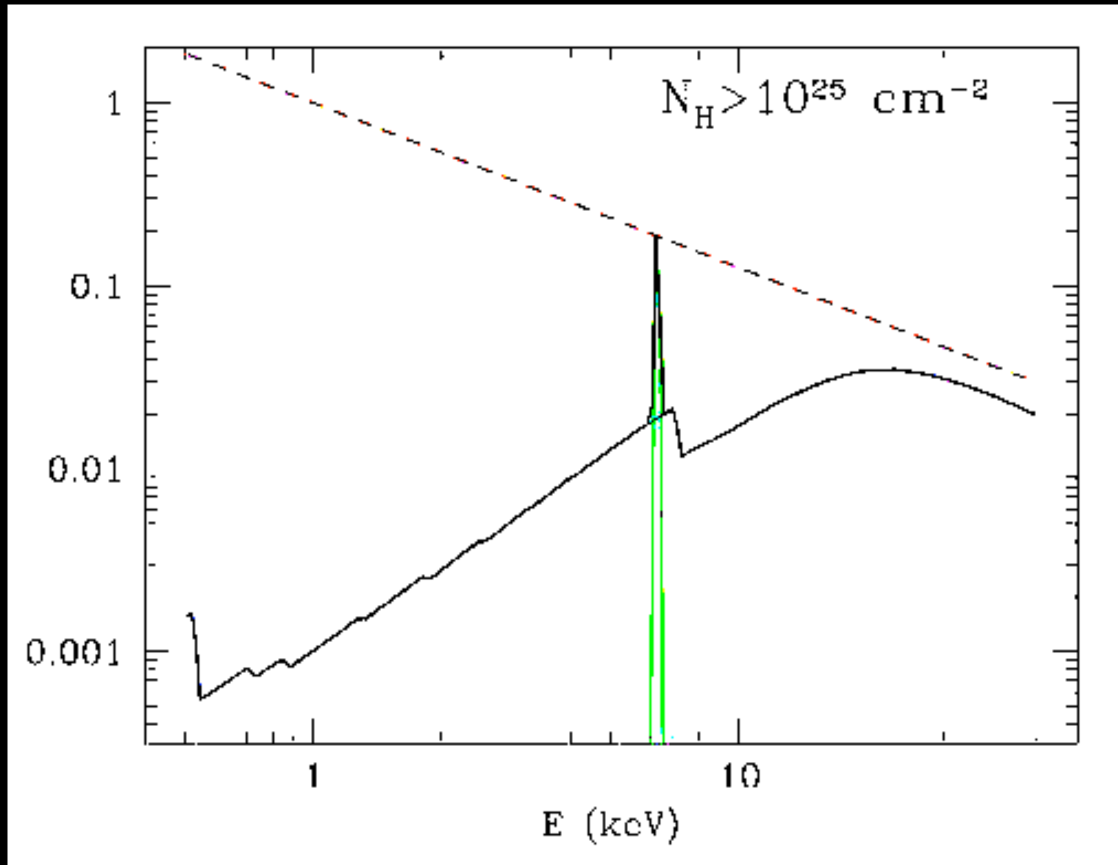

Cold absorber

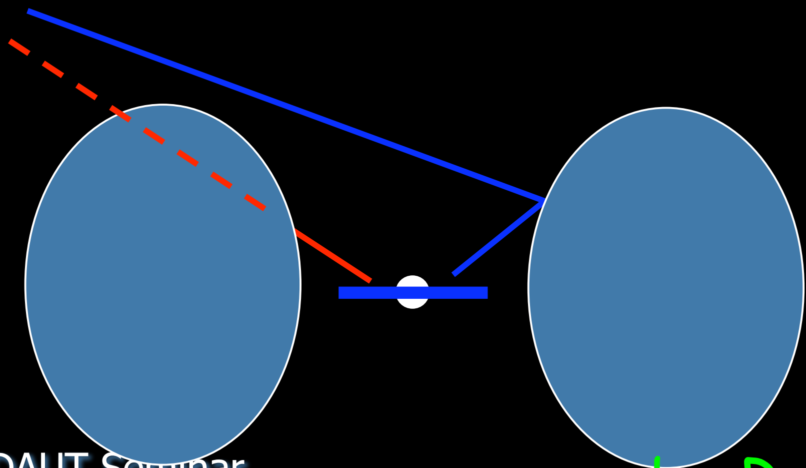

by R. Maiolino

Spectra extraction

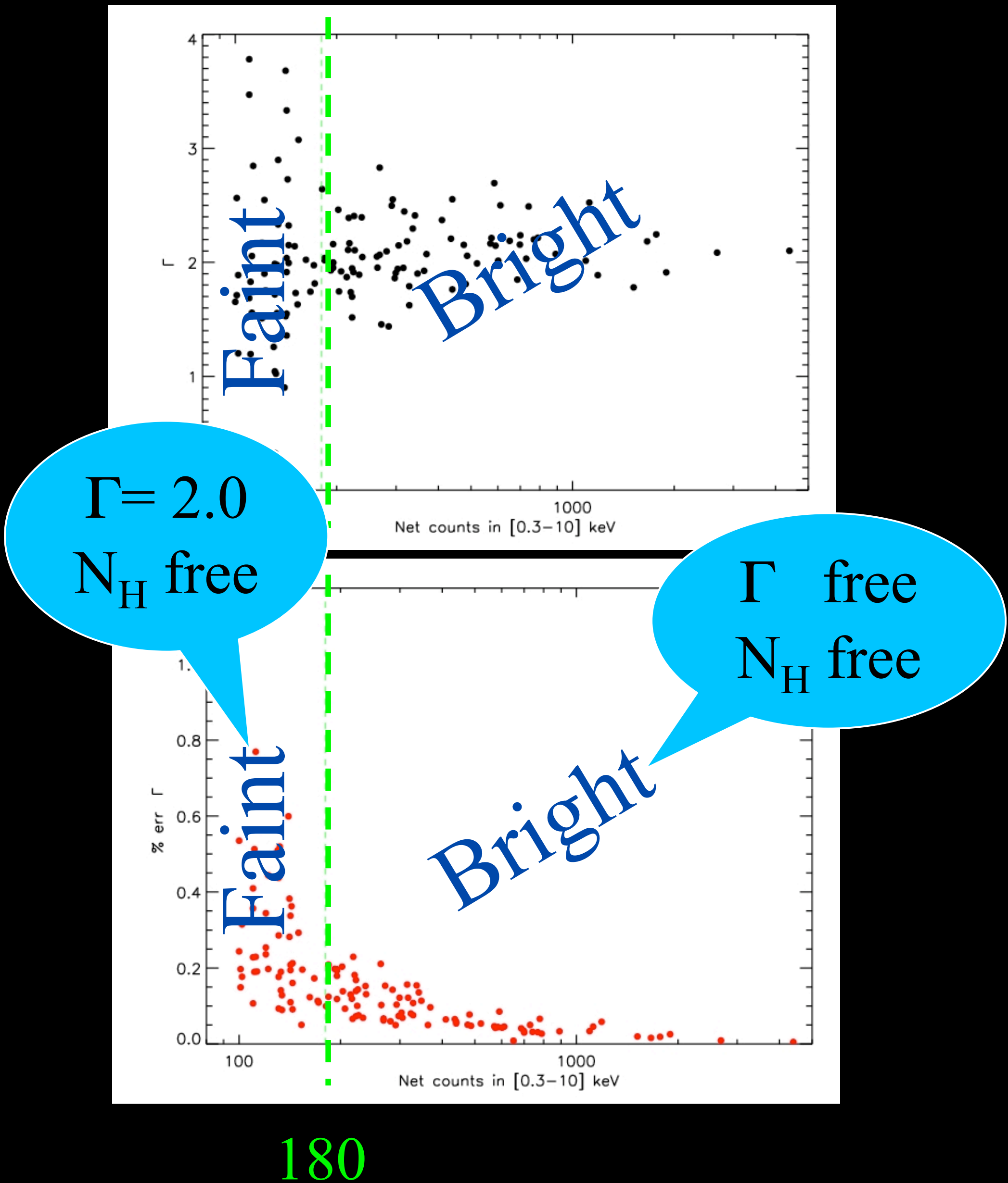

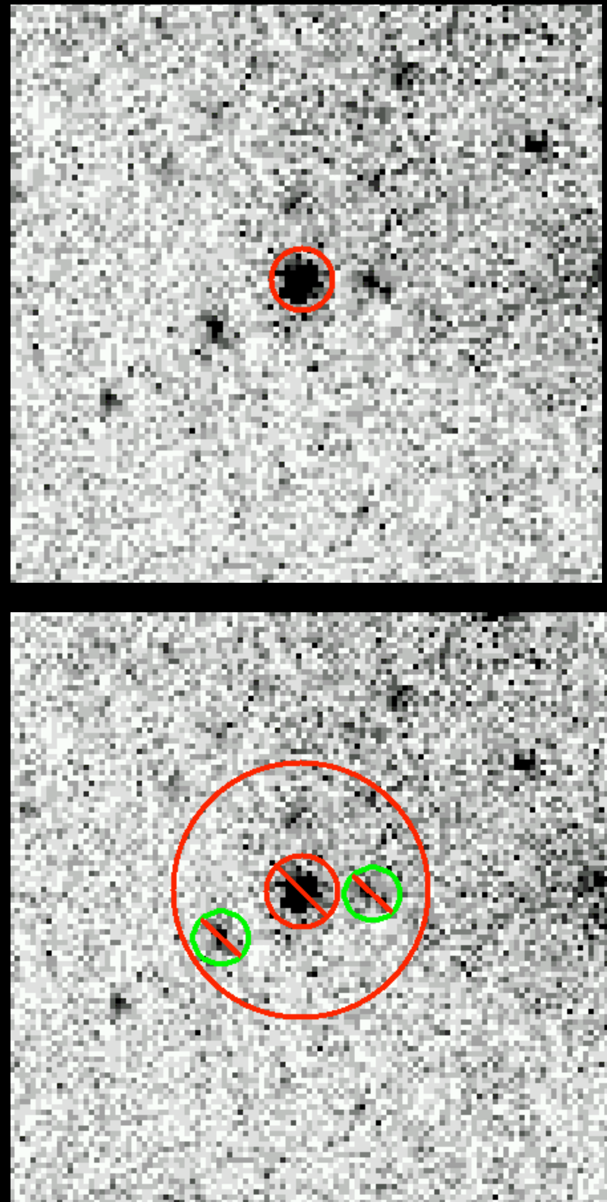

See also Tozzi et al. 2006

X-ray zoo

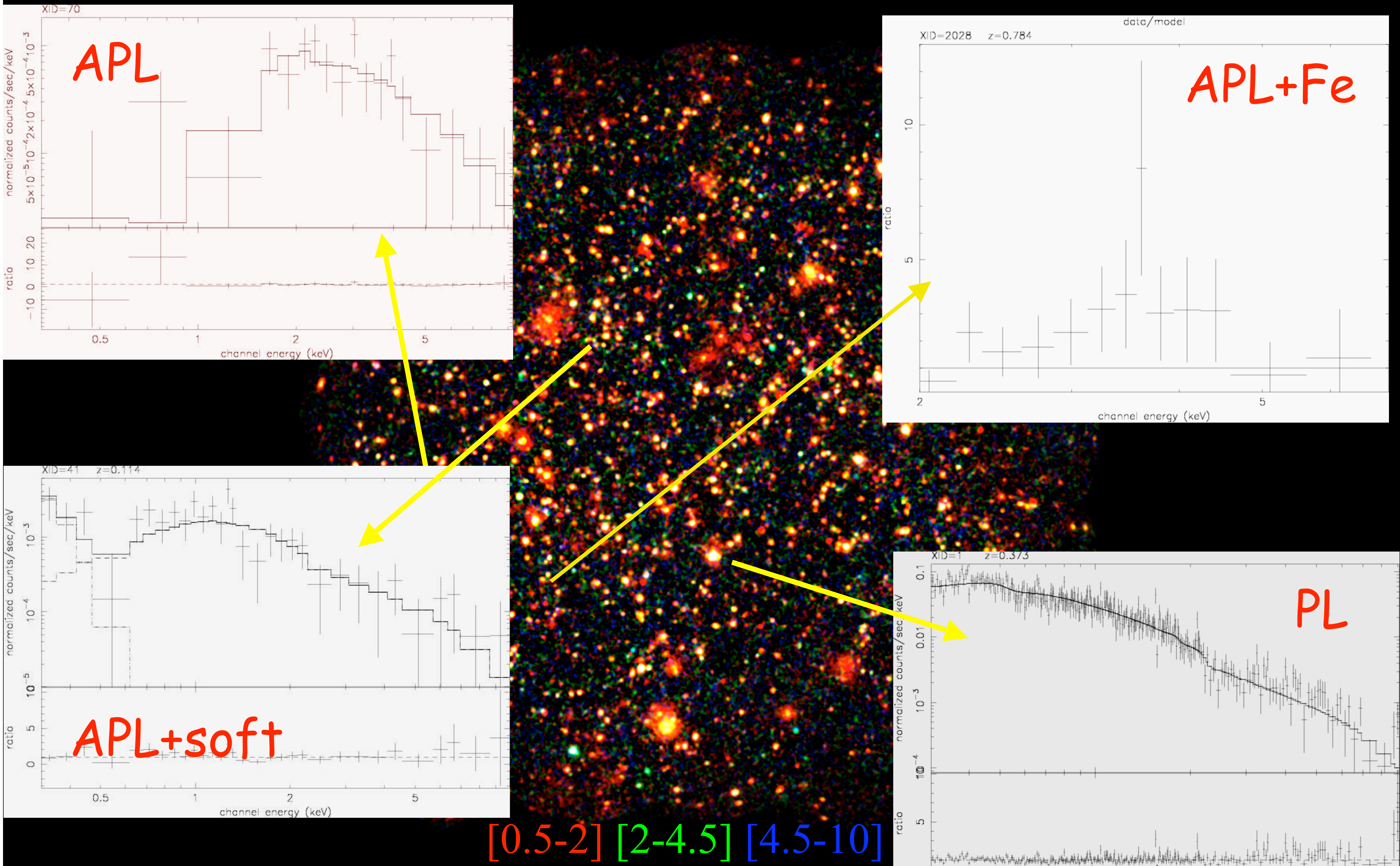

APL
XID=70
normalized counts/sec/keV
ratio
channel energy (keV)
APL+Fe
data/model
XID=2028 z=0.784
ratio
channel energy (keV)
APL+soft
XID=41 z=0.114
normalized counts/sec/keV
ratio
channel energy (keV)
PL
XID=1 z=0.373
normalized counts/sec/keV
ratio
channel energy (keV)
[0.5-2] [2-4.5] [4.5-10]

Γ vs N_H

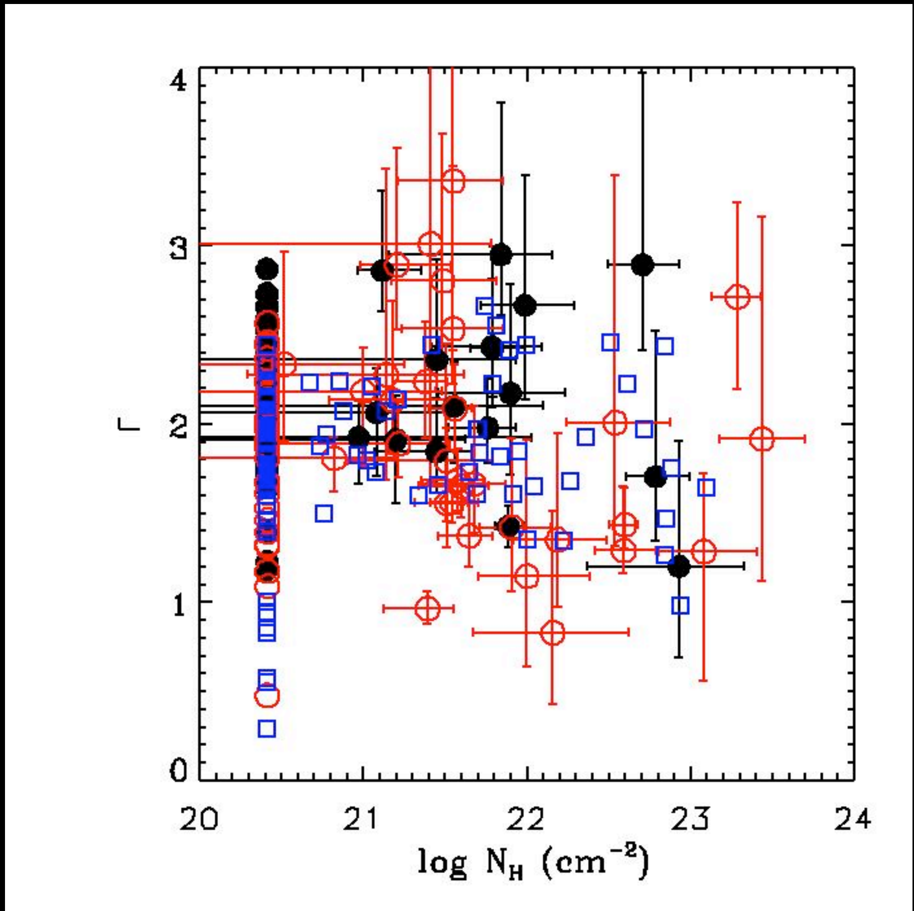

- $<\Gamma> = 2.06 \pm 0.08$
- $<\Gamma>$ does not change with N_H
- $<\Gamma>$ does not change with z

N_H^{gal}=[2.5-2.9] x 10^{20} cm^{-2}

N_H distribution

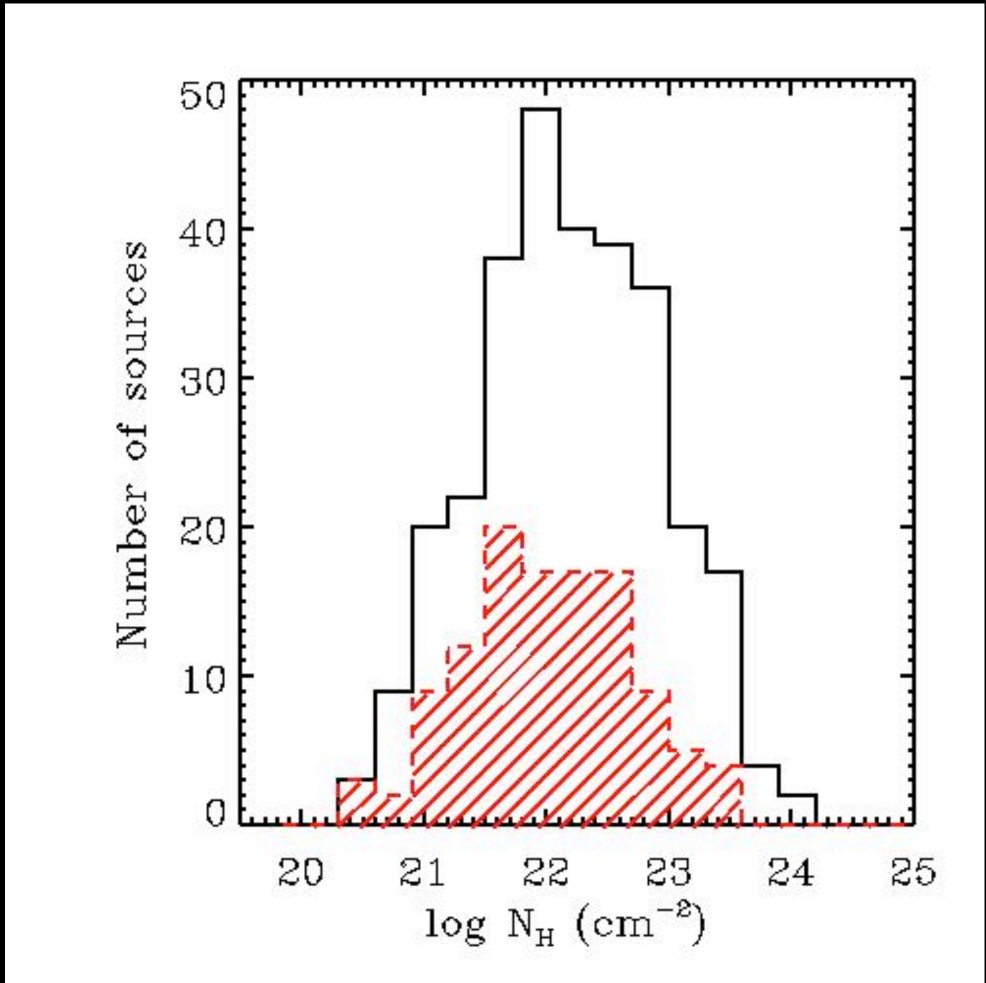

135 fits - 32 absorbed - 24%
431 fits - 116 absorbed - 27%
900 fits - 297 absorbed - 33%

Comparison between X-ray and optical classification

X-ray unabsorbed

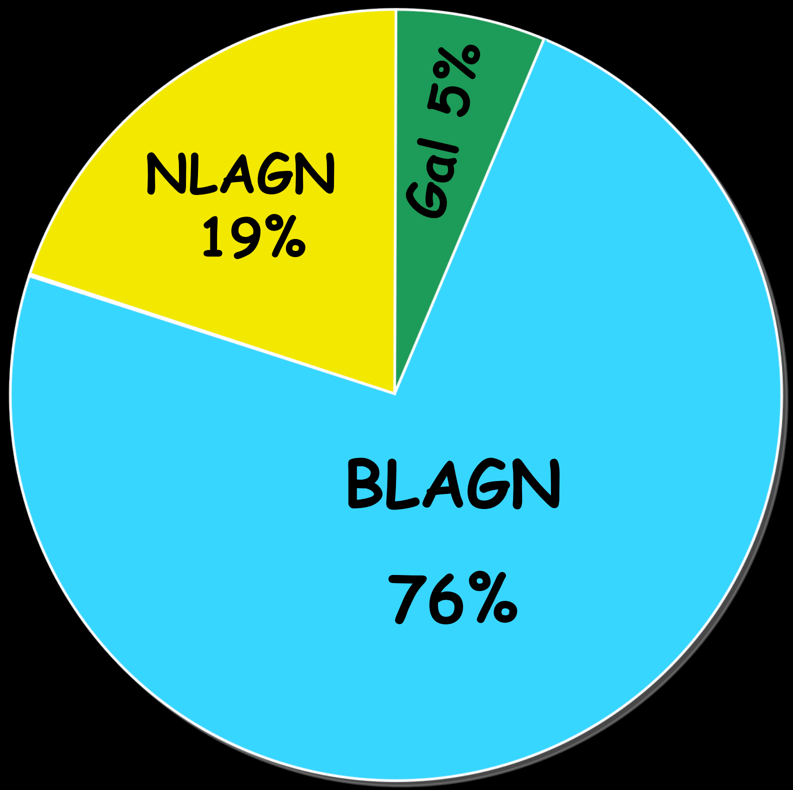

X-ray absorbed

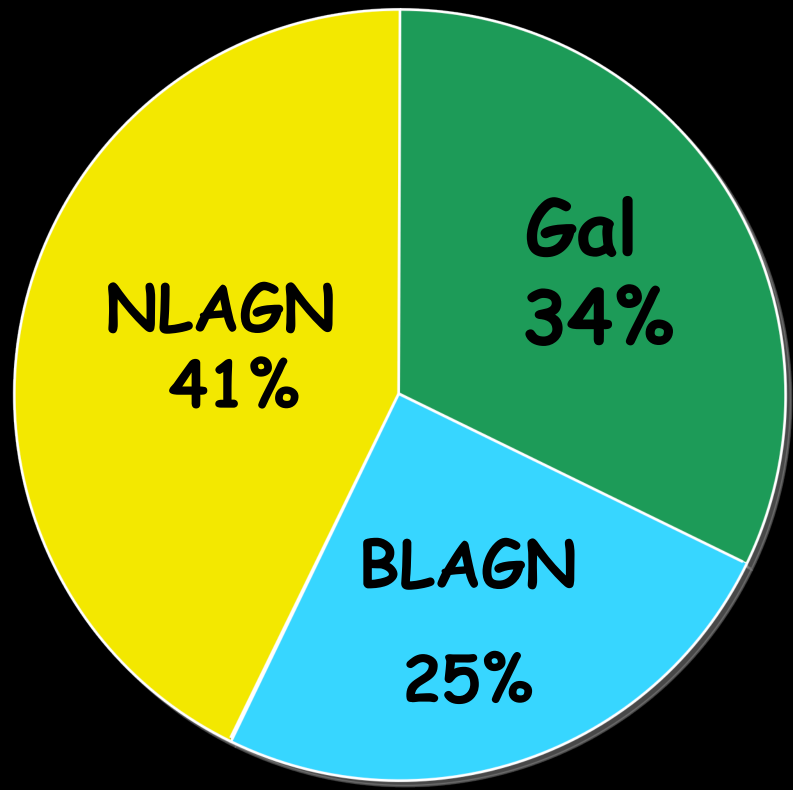

2/3of NLAGN do not show X-ray absorption:

80% z>0.4 --> Hα outside

50% have MgII inside but not enough S/N

X/O vs NH

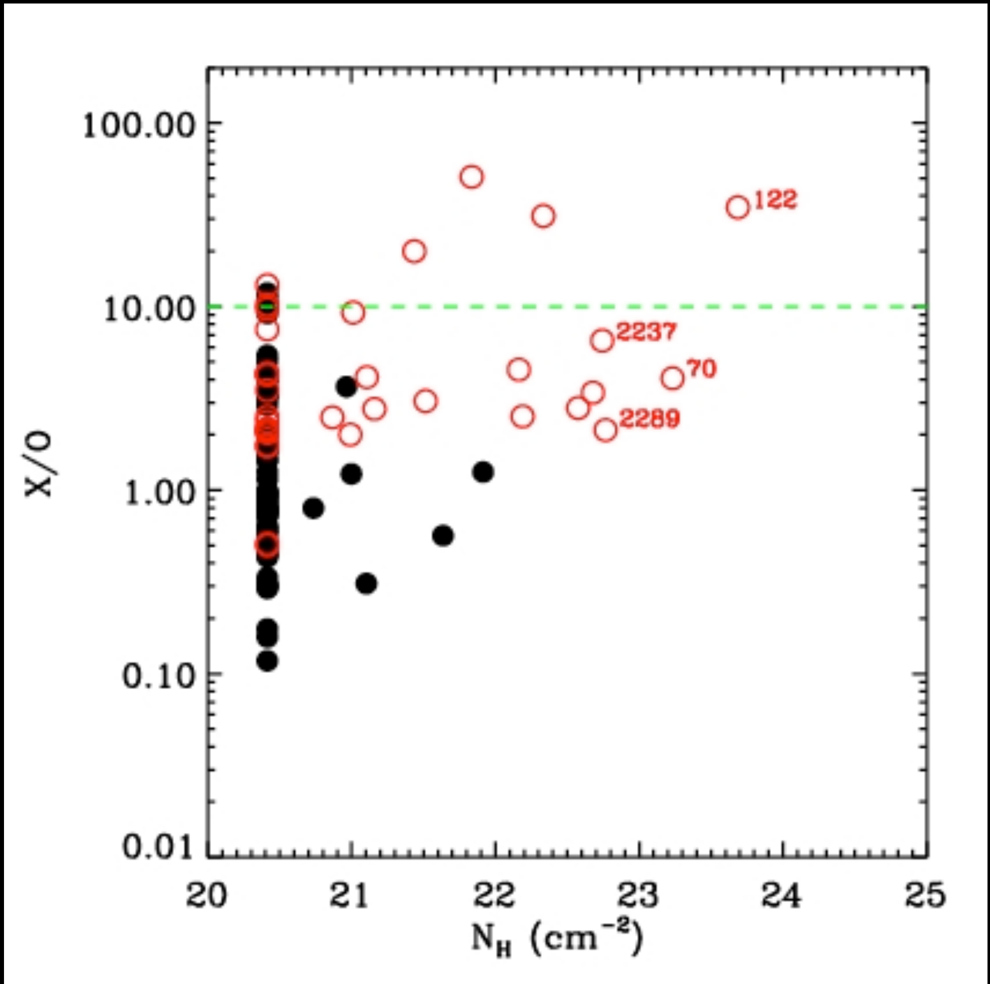

A tool to select obscured AGN:

60% X/O>10 are obscured
(to be compare with the 23% for the full sample)

High-z candidates?

QSO-2 candidates

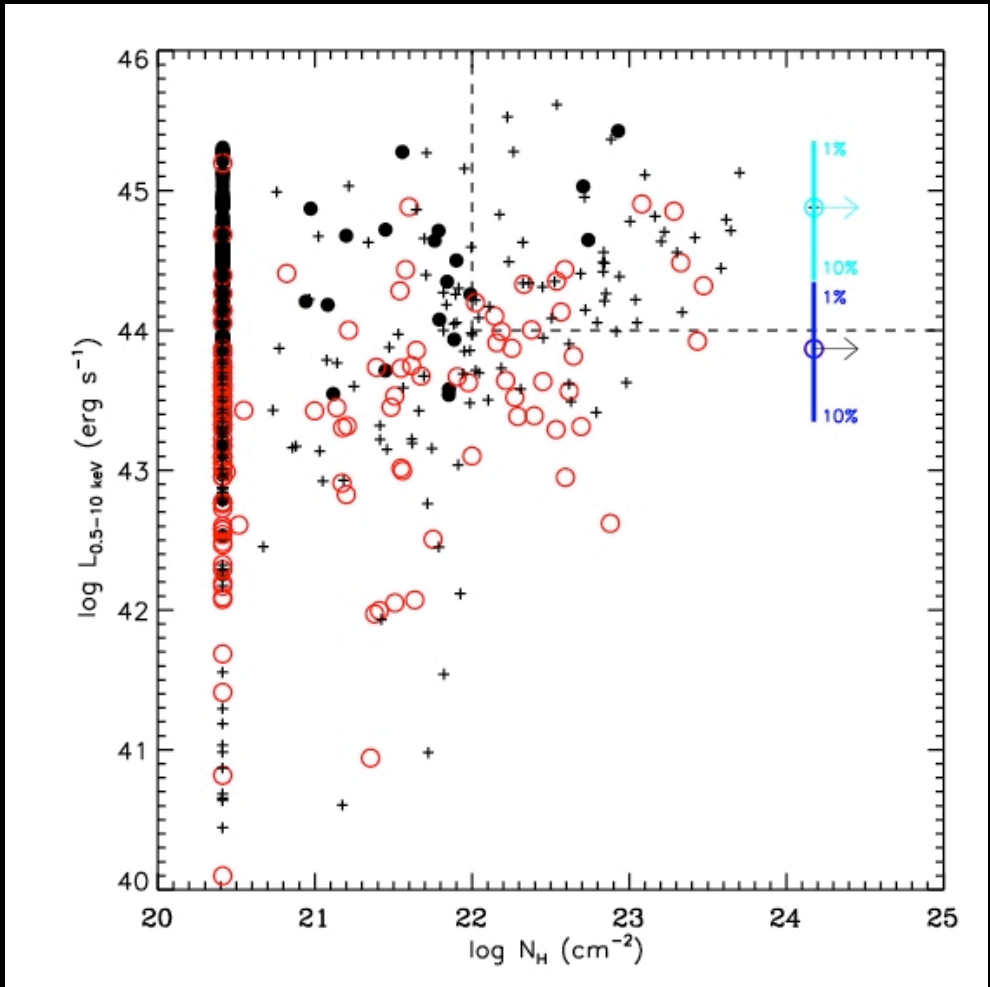

X-ray surveys are finding the radio quiet population of QSO-2

They are spanning a large redshift range: [0.6-2.8]

R-K ~ 4-5 (Vega)

Two are detected at 20cm:
540±24 μJy -> 9.8×10^{23} W/Hz
52±11 μJy -> 1.5×10^{23} W/Hz

For the other two:
$F_{20cm}(4.5\sigma) \sim 50$ μJy

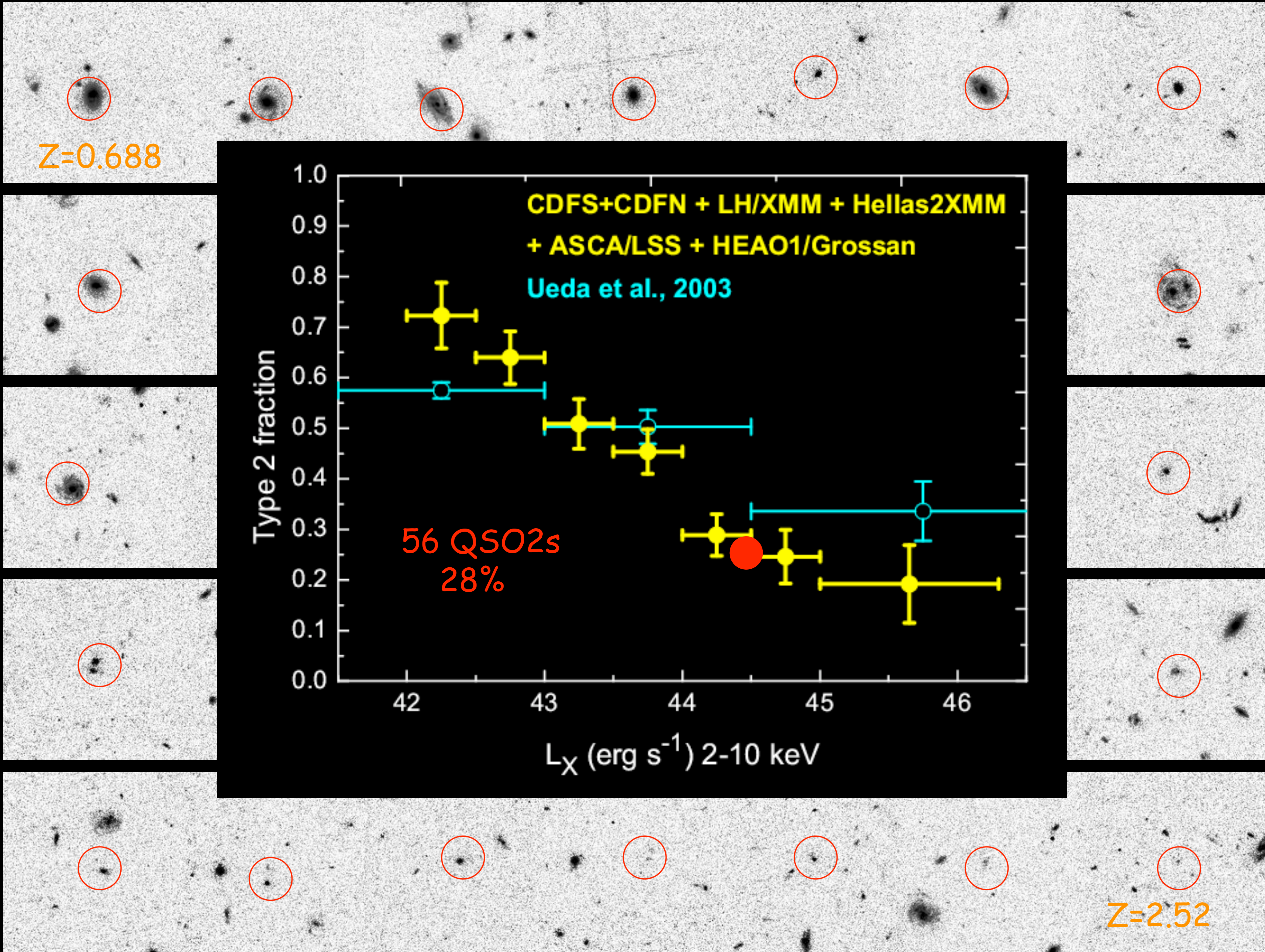
Z=0.688
Z=2.52
CDFS+CDFN + LH/XMM + Hellas2XMM
+ ASCA/LSS + HEAO1/Grossan
Ueda et al., 2003
56 QSO2s
28%
Type 2 fraction
1.0
0.9
0.8
0.7
0.6
0.5
0.4
0.3
0.2
0.1
0.0
42
43
44
45
46
L_X (erg s^{-1}) 2-10 keV

Composite Sy2

xid=122

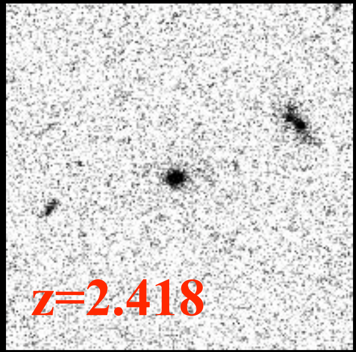

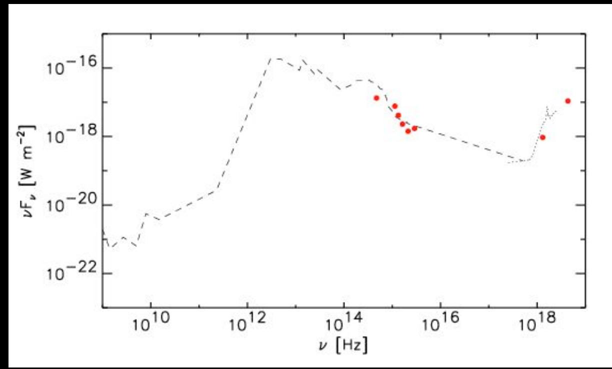

xid=70

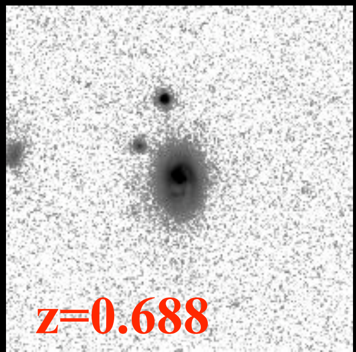

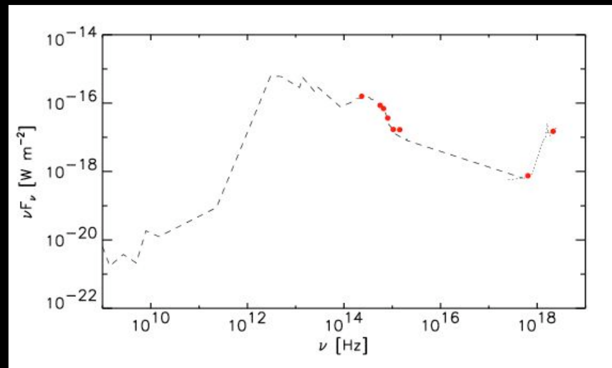

xid=2237

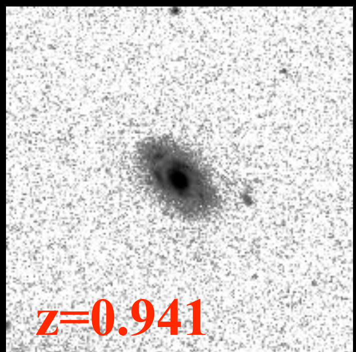

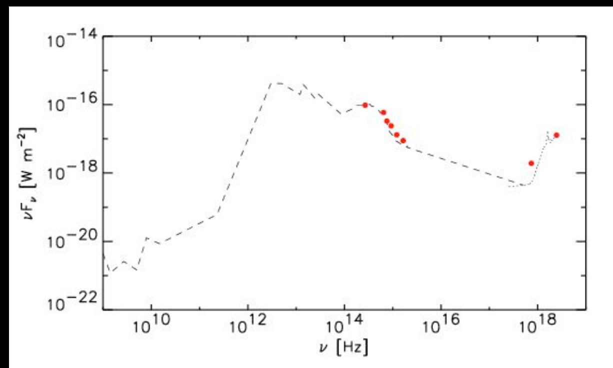

Compton-thick

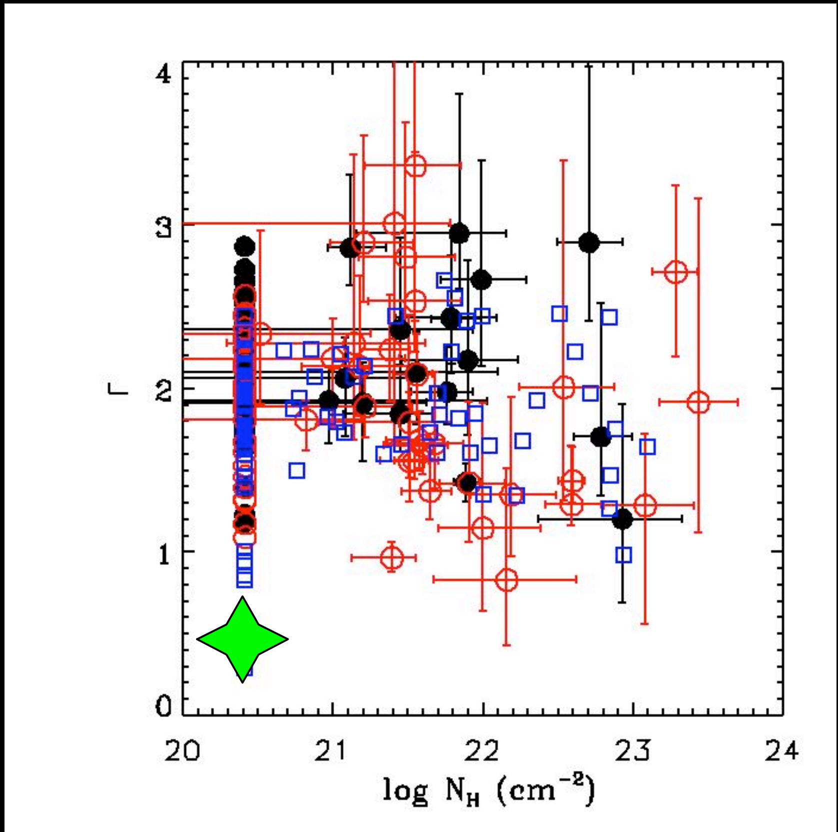

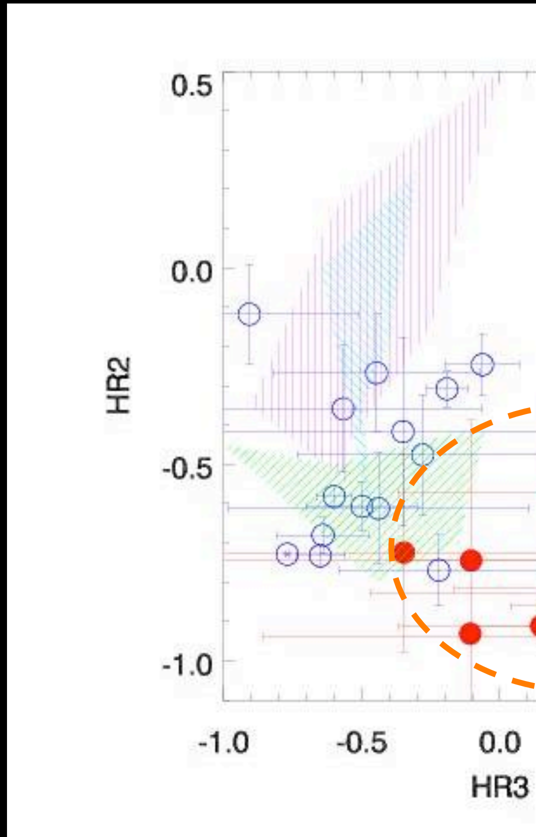

Hasinger et al. 2006

Guainazzi, Matt & Perola 2005

Local (z=0) sample of Compton thick sources

Compton-thick

25 arcsec

ACS/HST

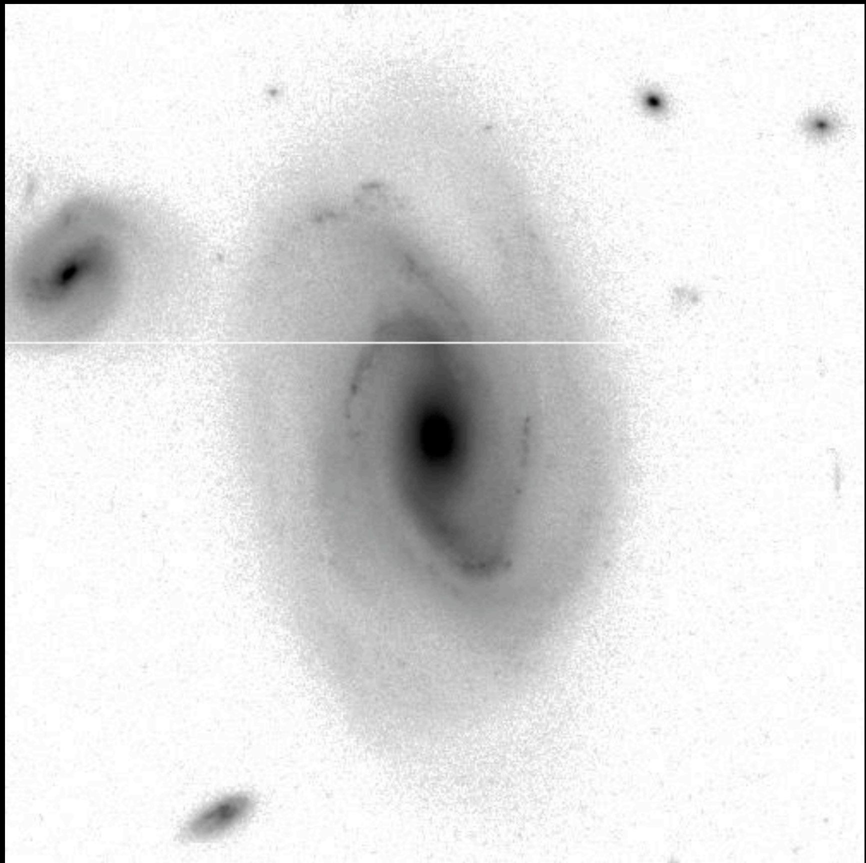

z=0.1248 (SDSS spectrum)

pexrav+gauss

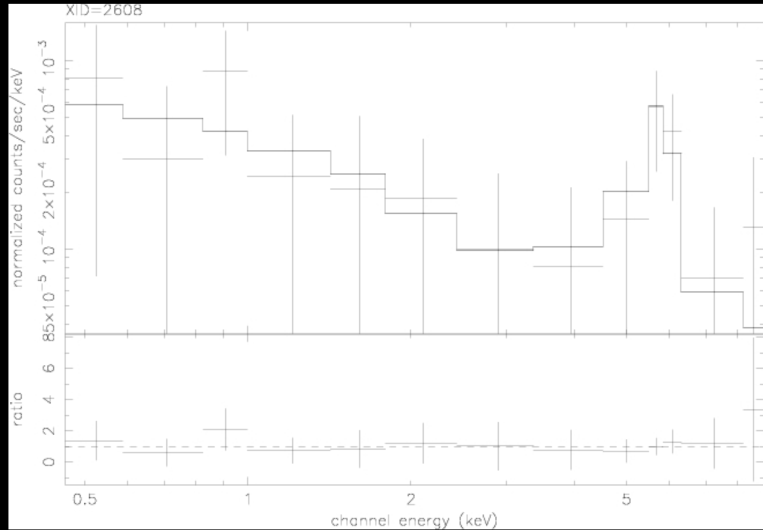

Table 3. Parameters of the best fit model for source xid 2608

Model[a]	Γ	N_H[b]	EW[c]	χ^2	d.o.f.
APL	2.0	$0.16^{+0.75}_{-0.16}$		9.3	11
pexrav	2.0			4.1	9
pexrav+gauss	2.0		792^{+1151}_{-493}	1.7	7

[a]Best fit model: *APL* = absorbed power-law; *pexrav* = pure reflection model; *pexrav+gauss* = pure reflection model plus a Gaussian line.

[b]Hydrogen column density in unit of 10^{22} cm^{-2}.

[c]Equivalent width of the Fe Kα line expressed in eV.

Compton-thick

25 arcsec

ACS/HST

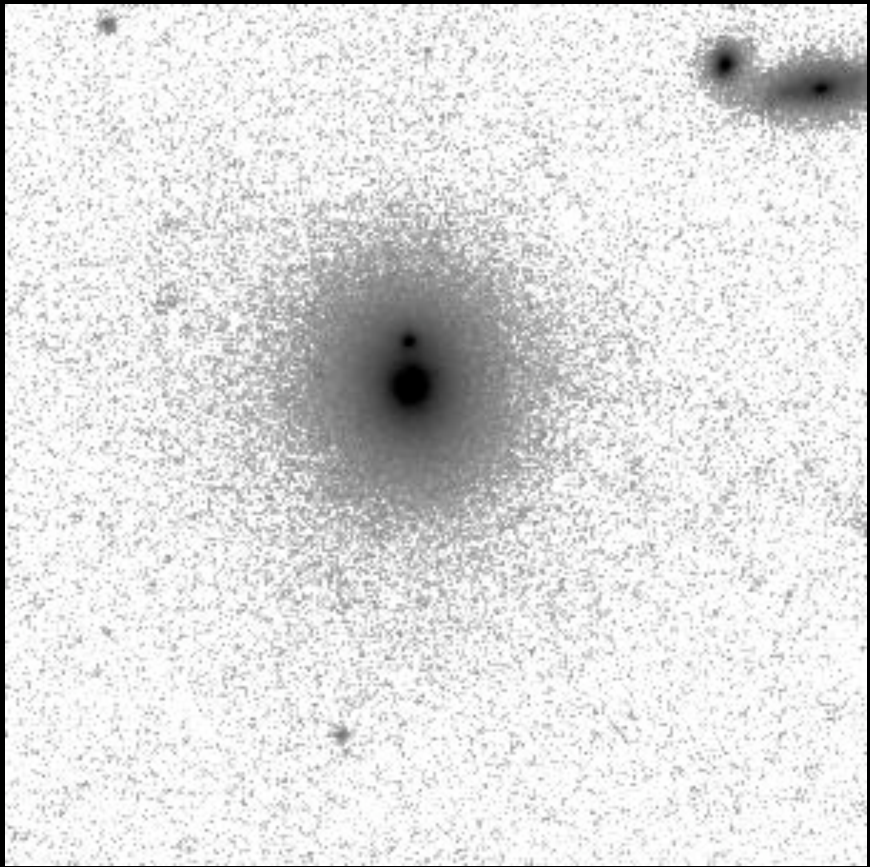

zphot=0.43

pexrav+gauss

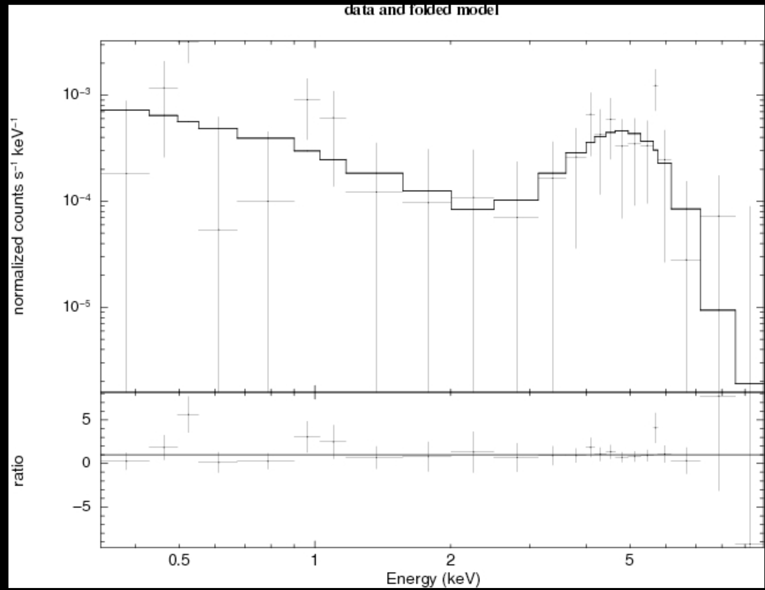

$EW_{FeK\alpha} = 1023^{1400}_{600}$ eV

Fe K line stacking

Method: the continuum is estimated for individual sources and subtracted, the residuals after correcting for the instrumental response curve are added together to form a stacked line profile. Spectral binning was designed to match a fixed rest-frame 200eV intervals.

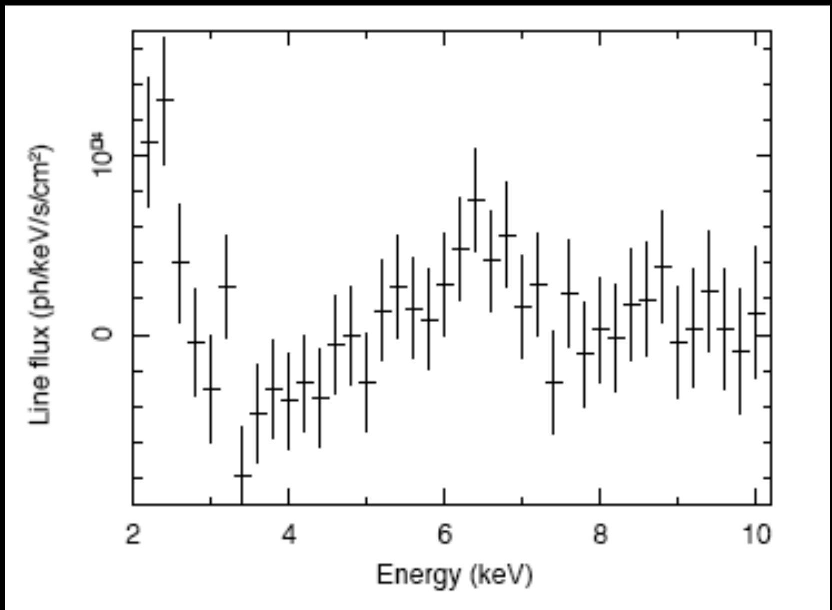

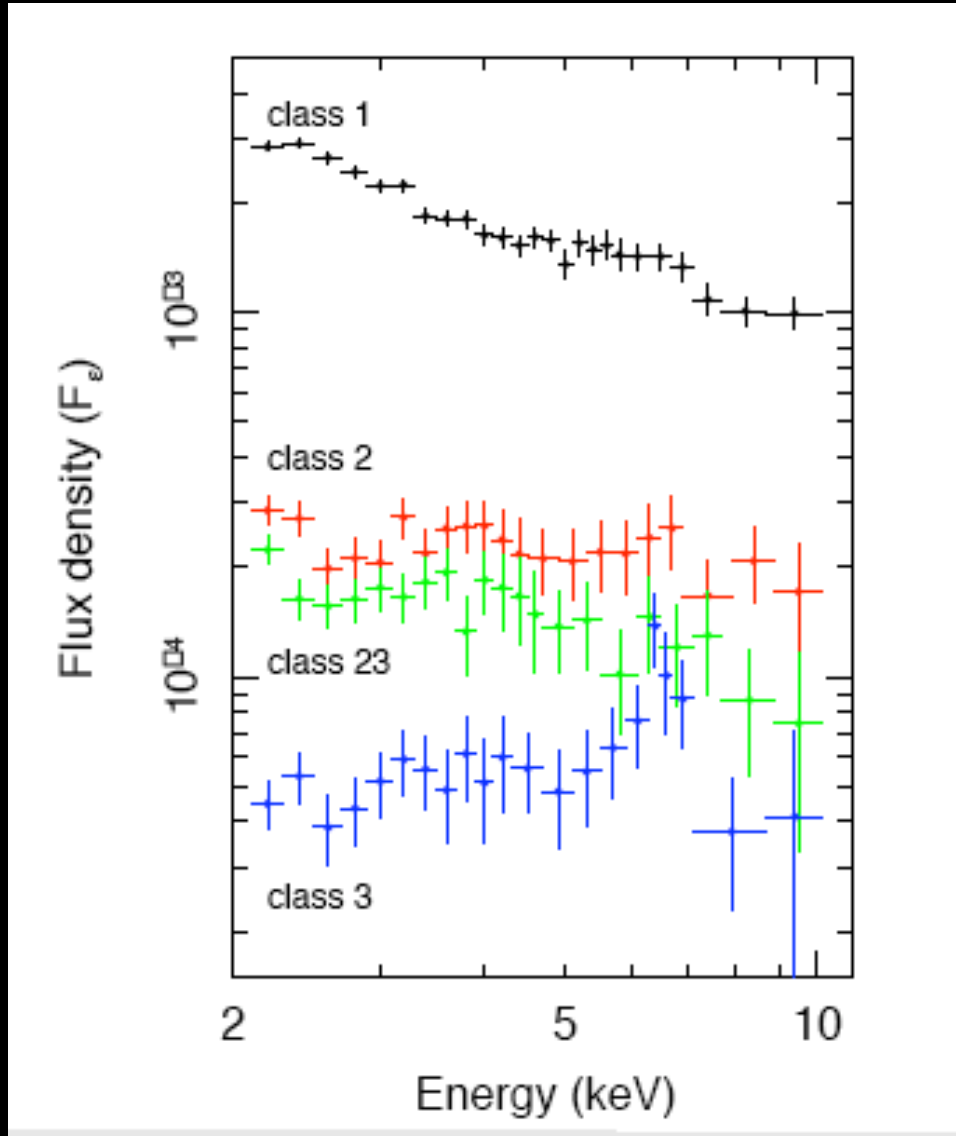

Iwasawa et al., in prep

combining R-K and X/O

X/O correlates with R-K
→combine these 2 criteria to isolate most obscured (QSO2) sources

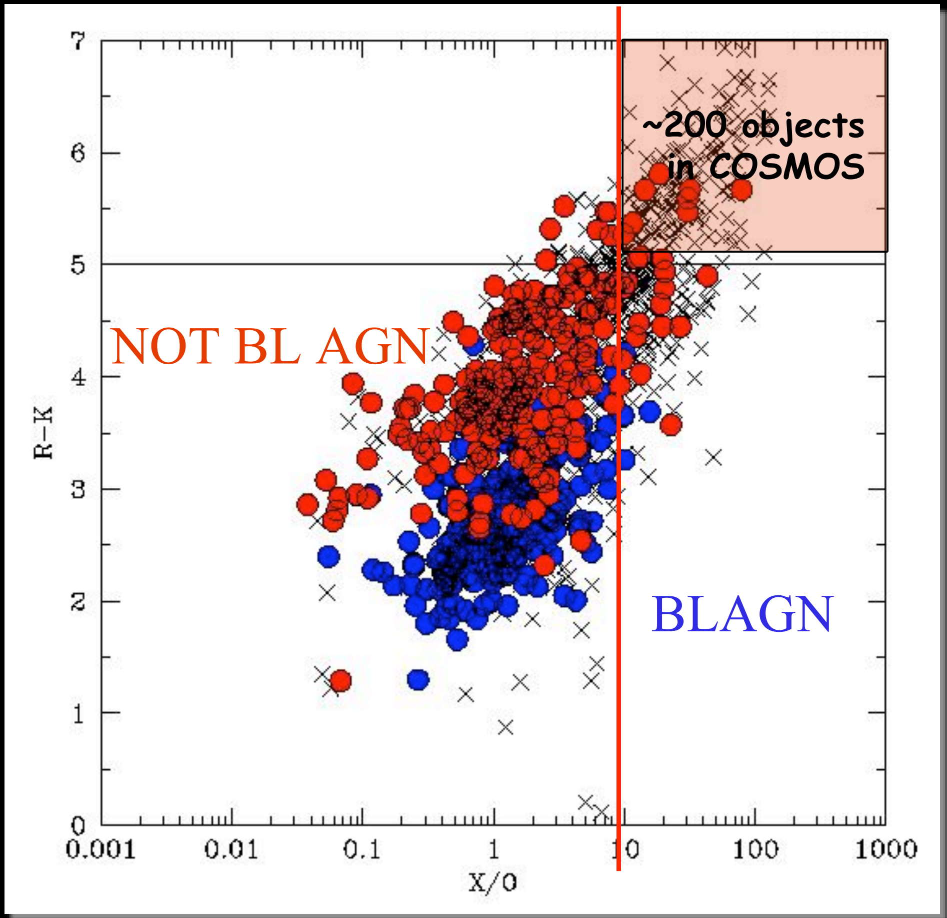

Civano et al. in preparation

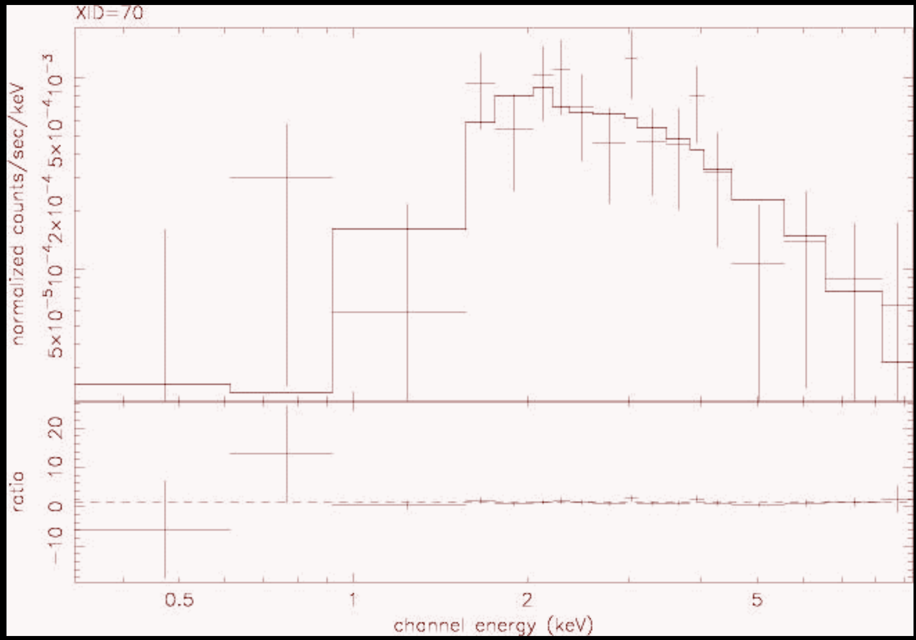

Mainieri et al. 2007

QSO2:

$N_H \sim 10^{23}$ cm^{-2}
$L_{2\text{-}10\,keV} = 5\times10^{44}$ erg/s
z(phot)=1.2

Where are X-ray sources in MIR diagrams?

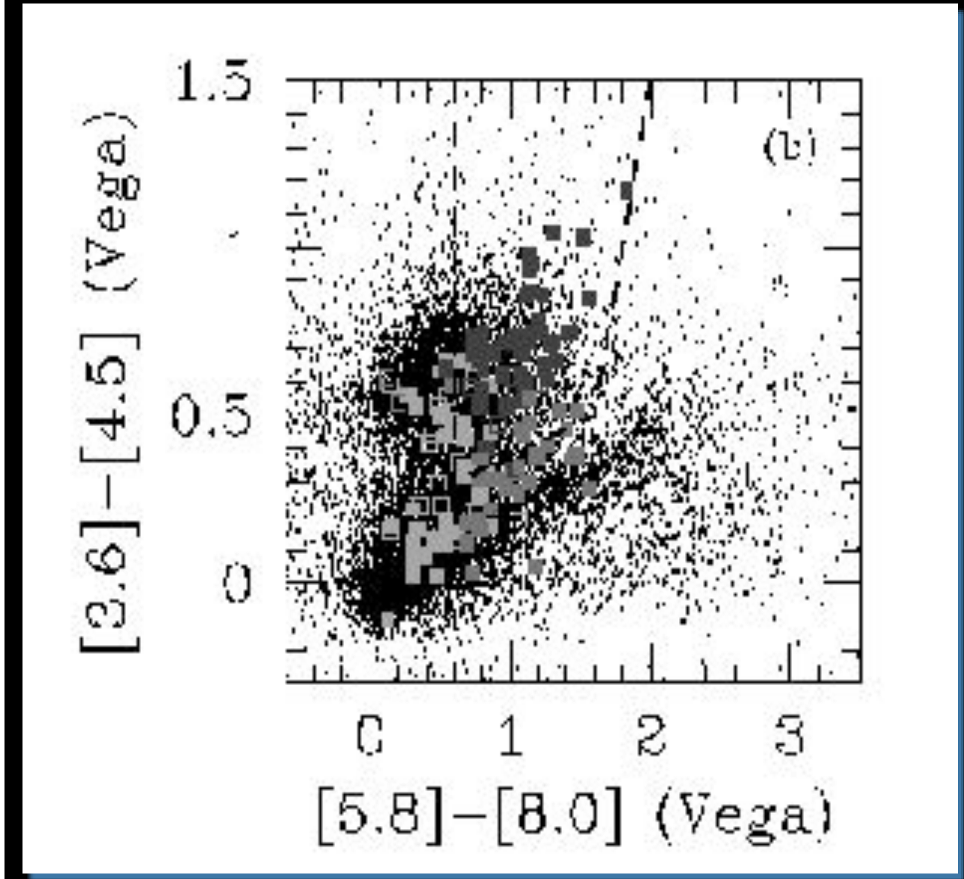

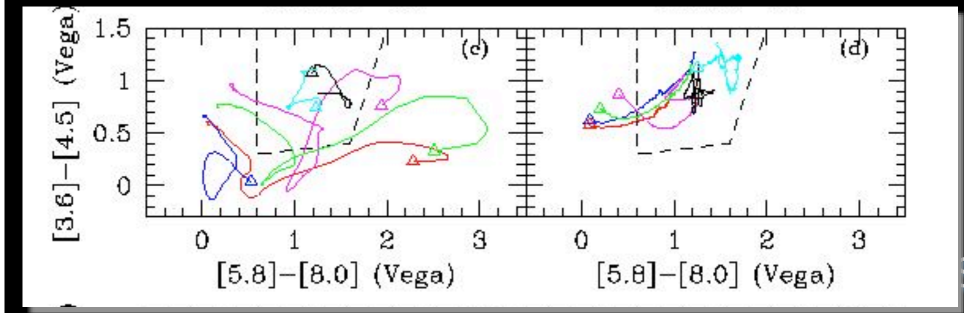

-51% of all the X-ray sample
-9% of all IRAC sample

Tracks of elliptical, Scd, Arp220, M82, NGC1068 (black), NGC5506 at z=0-2 and z=2-7

AGN → @any z
Starbursts → in & out
Elliptical → in at z>2

IRAC colors of X-ray sources

IRAC colors of identified (mostly low-z) **NOT BL AGN** show significant contribution
from host galaxy light → 50% outside

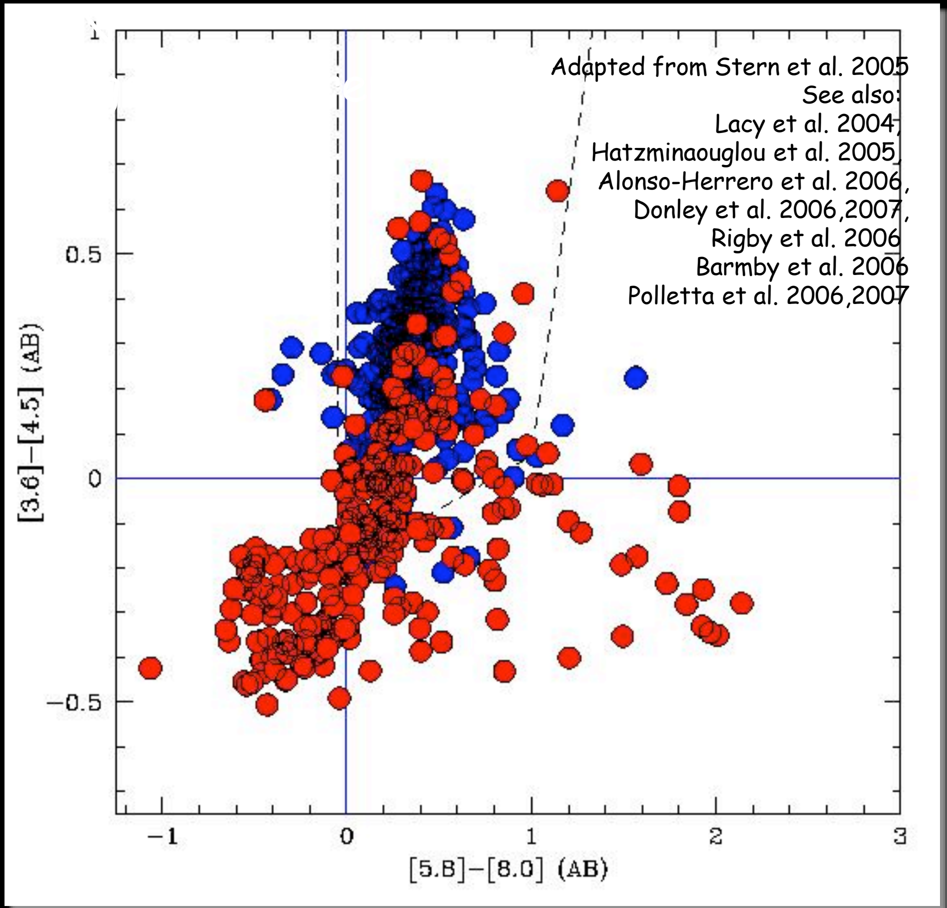

Fraction of AGN outside the wedge increases with decreasing X-ray flux
Population of obscured AGN at z~2 emerges at the faintest fluxes

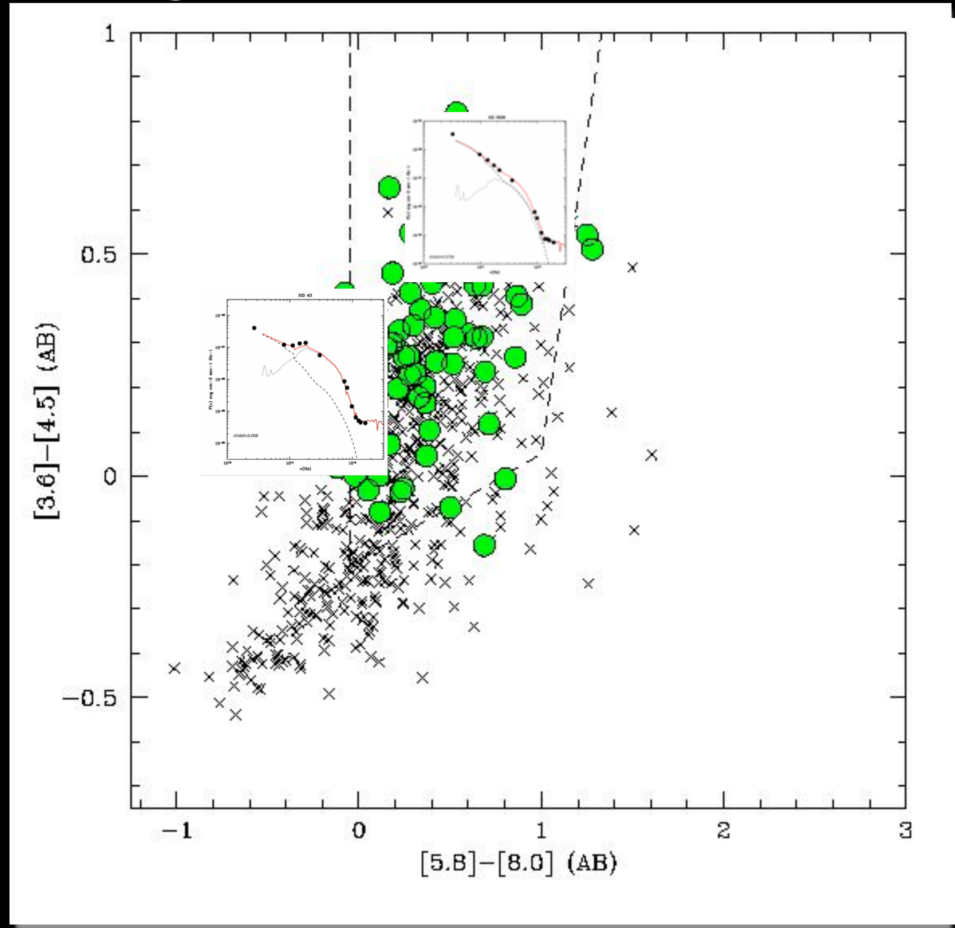

See also Hickox et al. 2007 from Bootes survey

Going at longer wavelength..

24micron/optical (MIR/O) flux ratio for obscured, X-ray selected sources correlate with R-K

HERE: MIPSO

MIPS shallow data, 0.3 mJy limit

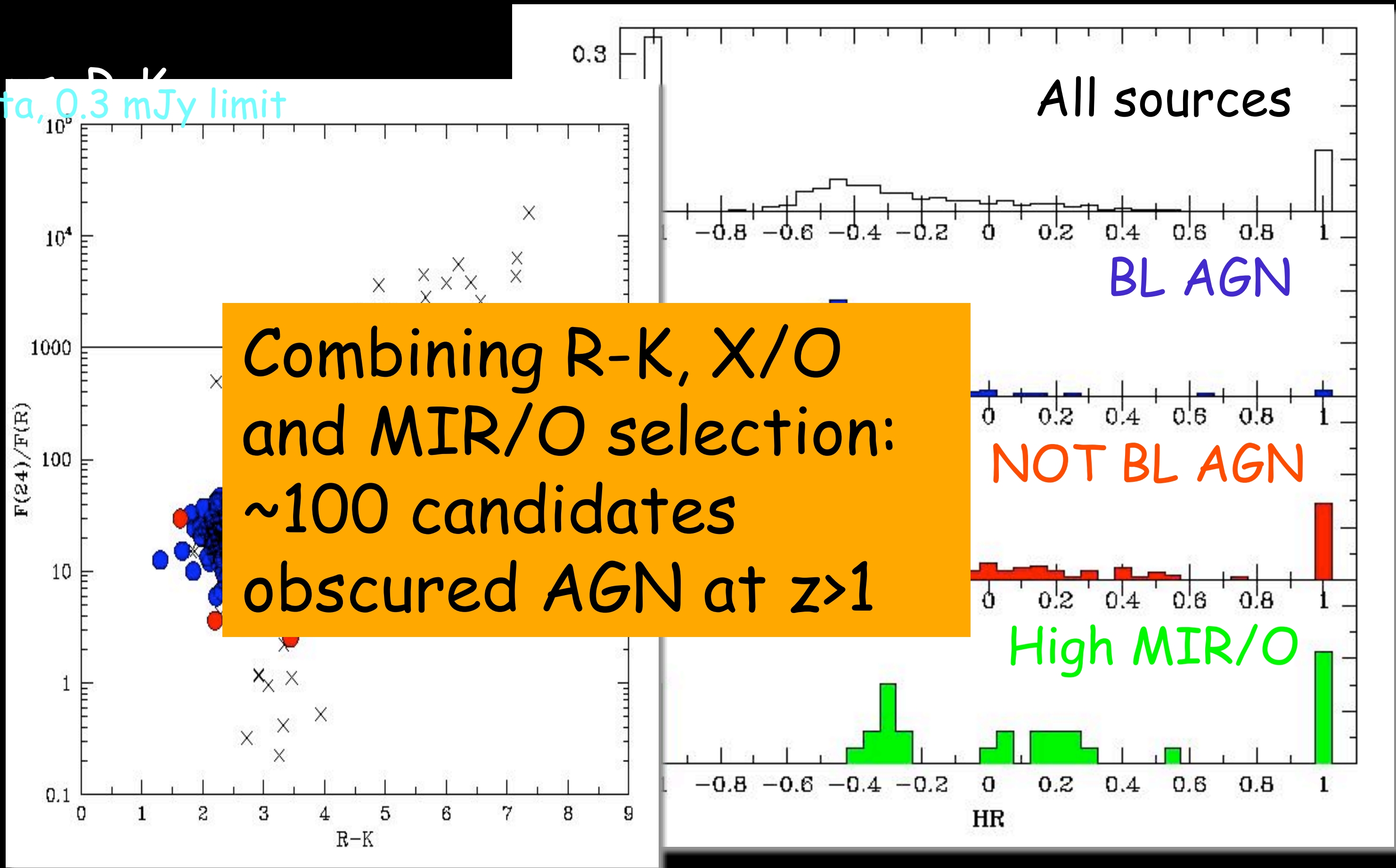

Combining R-K, X/O and MIR/O selection: ~100 candidates obscured AGN at z>1

Adapted from Fiore et al. 2007; see also Martinez-Sansigre et al. 2005, Houck et al. 2005, Yan et al. 2006, Daddi et al. 2007, Magliocchetti et al. 2007

Combining MIR/O and R-K criteria: selection of CT AGN at z~2

GOODS CDFS field

Stack of Chandra images excluding X-ray detections in two different MIR/O and R-K bins

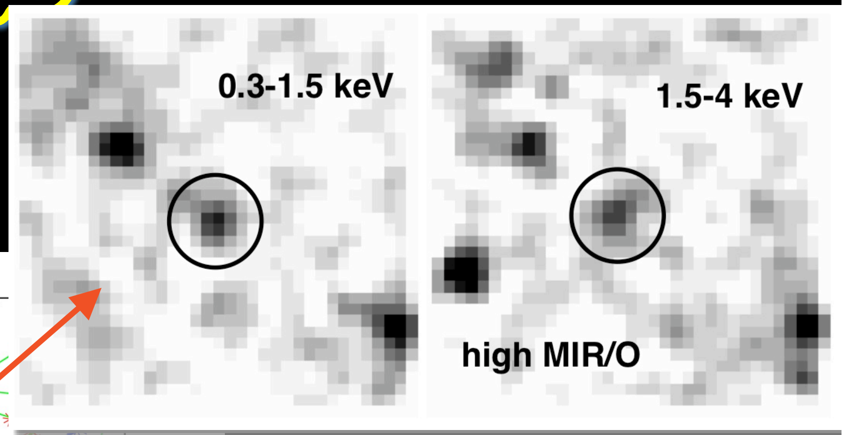

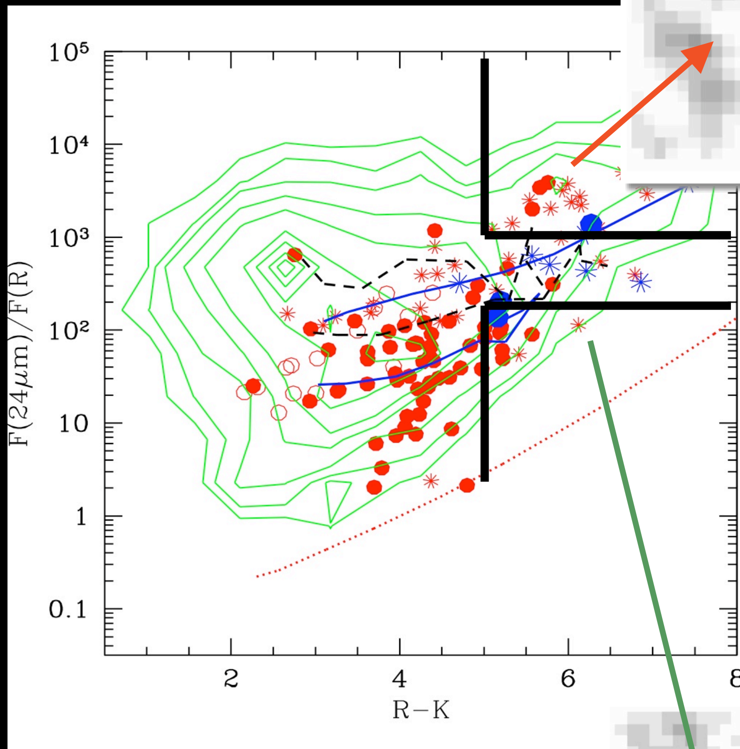

Stacked signal implies (unobs) Lx>43, NH>23 → Compton Thick

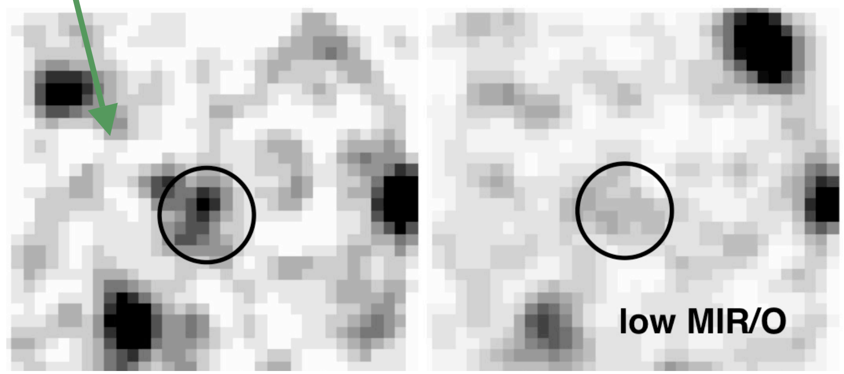

Fiore et al. 2007

See also Daddi et al. 2007

Summary

- C-thin AGN: hard X-ray surveys are quite effective, COSMOS has an excellent X-ray coverage (XMM+Chandra) and spectroscopic follow-up
- A large population of QSO-2, the observed number density is in agreement with the decrease of the type-2/type-1 with X-ray luminosity
- C-thick: hard X-ray surveys miss a large fraction of them
  - move to longer wavelength: X-ray + mid-IR
    - SED of obscured sources are not always PL in IRAC (caution on using IRAC only colors diagram to select obscured AGN)
  - extremely deep XMM exposure (not confusion limited in the 5-10 keV band)
  - future missions (Simbol-X, [0.5-80] keV)

X-ray spectral properties catalogue

Table 4—Continued

IAU[a]	XID[b]	RA[c] (J2000)	Dec[c] (J2000)	counts[d] [0.3-10]	z[e]	MODEL[f]	Γ	N_H	fx[g] [0.5-2]	fx[g] [2-10]	fx[g] [0.5-10]	L_X[h] [0.5-2]	L_X[h] [2-10]	L_X[h] [0.5-10]
XMMC_J100129.41+013633.7	2021	10:01:29.41	1:36:33.75	271	0.104	APL	$1.46^{1.73}_{1.23}$	$22.42^{22.55}_{22.29}$	77.20	1764.50	1841.70	42.15	42.75	42.85
XMMC_J100211.31+013707.2	2028	10:02:11.31	1:37:07.15	293	0.784	APL+Fe	$2.55^{2.79}_{2.29}$	$21.83^{21.95}_{21.69}$	113.12	204.74	317.86	43.75	43.50	43.94
XMMC_J100257.55+015405.6	2036	10:02:57.55	1:54:05.58	233	0.971	PL	$1.90^{2.05}_{1.76}$	......	81.37	113.86	195.23	43.56	43.71	43.94
XMMC_J100033.51+013812.6	2040	10:00:33.51	1:38:12.61	317	0.520	APL	$2.45^{2.83}_{2.15}$	$20.57^{21.09}_{20.42}$	158.53	106.61	265.15	43.25	43.05	43.46
XMMC_J100237.09+014648.3	2043	10:02:37.09	1:46:48.33	347	0.668	APL+Fe	$1.70^{1.90}_{1.51}$	$21.81^{21.93}_{21.67}$	56.18	171.00	227.18	43.23	43.53	43.70
XMMC_J100303.04+015209.2	2046	10:03:03.04	1:52:09.19	341	1.800	PL	$2.25^{2.45}_{2.07}$	......	51.66	44.97	96.63	44.06	44.00	44.33
XMMC_J100151.19+020032.8	2058	10:01:51.19	2:00:32.81	779	0.964	APL	$2.10^{2.19}_{1.97}$	$20.44^{21.02}_{20.42}$	110.01	121.24	231.25	43.78	43.82	44.10
XMMC_J100229.27+014528.2	2071	10:02:29.27	1:45:28.21	328	0.876	PL	$1.63^{1.78}_{1.50}$	......	52.54	107.29	159.83	43.21	43.52	43.69
XMMC_J100141.42+021031.8	2078	10:01:41.42	2:10:31.78	195	0.982	APL	$2.00^{2.26}_{1.64}$	$21.05^{21.52}_{20.42}$	50.07	67.61	117.68	43.45	43.55	43.81
XMMC_J100238.78+013938.2	2080	10:02:38.78	1:39:38.25	238	1.315	PL	$1.88^{2.03}_{1.74}$	......	82.12	120.83	202.95	43.89	44.05	44.28
XMMC_J100238.27+013747.8	2093	10:02:38.27	1:37:47.75	222	2.506	PL	$1.98^{2.18}_{1.80}$	......	75.99	98.66	174.65	44.58	44.69	44.94
XMMC_J100214.21+020620.0	2096	10:02:14.21	2:06:20.02	482	1.265	APL	$1.81^{1.95}_{1.67}$	$21.15^{21.48}_{20.42}$	71.46	125.86	197.32	43.71	43.93	44.14
XMMC_J100219.58+015536.9	2105	10:02:19.58	1:55:36.94	323	1.509	PL	$2.20^{2.45}_{1.97}$	......	48.68	45.39	94.07	43.85	43.82	44.13
XMMC_J100305.20+015157.0	2118	10:03:05.20	1:51:57.04	195	0.969	PL	$1.97^{2.27}_{1.69}$	......	65.36	86.40	151.77	43.50	43.62	43.87
XMMC_J095848.84+023442.3	2138	9:58:48.84	2:34:42.34	729	1.551	PL	$2.03^{2.14}_{1.92}$	......	51.39	61.83	113.22	43.90	43.98	44.24
XMMC_J100230.13+014810.0	2152	10:02:30.13	1:48:10.01	281	0.626	PL	$2.23^{2.58}_{1.92}$	......	37.60	33.63	71.22	42.79	42.74	43.07
XMMC_J100232.55+014009.5	2169	10:02:32.55	1:40:09.53	144	1.776	PL	2.00	......	45.21	54.98	100.19	43.99	44.07	44.34
XMMC_J100141.11+021259.9	2191	10:01:41.11	2:12:59.88	225	0.621	APL	$2.41^{3.07}_{2.06}$	$20.52^{21.33}_{20.42}$	33.06	23.99	57.05	42.81	42.65	43.04
XMMC_J100236.79+015948.5	2202	10:02:36.79	1:59:48.50	142	1.516	PL	2.00	......	44.66	53.86	98.51	43.81	43.90	44.16
XMMC_J100038.40+013708.4	2211	10:00:38.40	1:37:08.37	153	1.251	PL	2.00	......	36.29	45.60	81.88	43.52	43.62	43.87
XMMC_J100156.40+014811.0	2213	10:01:56.40	1:48:11.00	263	0.957	APL	$2.05^{2.33}_{1.62}$	$20.88^{21.55}_{20.42}$	20.73	25.40	46.14	43.02	43.08	43.35
XMMC_J100226.77+014052.1	2218	10:02:26.77	1:40:52.05	123	0.247	PL	2.00	......	36.16	43.97	80.13	41.83	41.91	42.17
XMMC_J100041.57+013658.7	2220	10:00:41.57	1:36:58.69	162	0.995	PL	2.00	......	39.58	48.47	88.05	43.31	43.40	43.66
XMMC_J100156.31+020942.9	2232	10:01:56.31	2:09:42.91	131	1.641	PL	2.00	......	18.01	22.62	40.63	43.51	43.60	43.86
XMMC_J100253.16+013457.8	2235	10:02:53.16	1:34:57.85	100	2.248	PL	2.00	......	26.30	31.85	58.15	44.00	44.09	44.35
XMMC_J095904.34+022552.8	2237	9:59:04.34	2:25:52.75	192	0.941	APL	$1.93^{2.55}_{1.54}$	$22.77^{22.98}_{22.59}$	19.18	127.42	146.60	43.65	43.80	44.03
XMMC_J100223.02+020639.5	2246	10:02:23.02	2:06:39.48	303	0.899	PL	$1.97^{2.24}_{1.72}$	......	38.35	56.49	94.85	43.24	43.36	43.60
XMMC_J100243.88+020501.6	2261	10:02:43.88	2:05:01.59	206	1.234	PL	$2.00^{2.30}_{1.74}$	......	26.34	33.25	59.59	43.36	43.47	43.72
XMMC_J100208.53+014553.7	2276	10:02:08.53	1:45:53.65	111	2.215	PL	2.00	......	16.88	21.21	38.09	43.80	43.90	44.15
XMMC_J100158.05+014621.7	2289	10:01:58.05	1:46:21.74	122	0.831	APL	2.00	$22.73^{22.94}_{22.50}$	8.02	51.79	59.81	43.18	43.28	43.53
XMMC_J100130.33+014305.0	2299	10:01:30.33	1:43:04.97	110	1.571	PL	2.00	......	18.86	23.69	42.55	43.48	43.58	43.83
XMMC_J100143.54+015606.2	2361	10:01:43.54	1:56:06.18	195	2.181	PL	$1.98^{2.27}_{1.72}$	......	28.50	36.14	64.64	44.01	44.11	44.36
XMMC_J100240.34+020146.4	2370	10:02:40.34	2:01:46.37	132	0.638	APL	2.00	$22.16^{22.64}_{21.75}$	11.08	32.35	43.43	42.68	42.77	43.02